Ocean Sci., 18, 1703–1724, 2022
https://doi.org/10.5194/os-18-1703-2022

Ocean Science
Open Access

Modelling floating riverine litter in the south-eastern Bay of Biscay: a regional distribution from a seasonal perspective

Irene Ruiz[1], **Anna Rubio**[1], **Ana J. Abascal**[2], **and Oihane C. Basurko**[1]

[1]AZTI, Marine Research, Basque Research and Technology Alliance (BRTA), Pasaia, 20110, Spain
[2]IHCantabria – Instituto de Hidráulica Ambiental de la Universidad de Cantabria, Santander, 39011, Spain

Correspondence: Irene Ruiz (iruiz@azti.es)

Received: 9 May 2022 – Discussion started: 18 May 2022
Revised: 7 October 2022 – Accepted: 26 October 2022 – Published: 5 December 2022

Abstract. Although rivers contribute to the flux of litter to the marine environment, estimates of riverine litter amounts and detailed studies on floating riverine litter behaviour once it has reached the sea are still scarce. This paper provides an analysis of the seasonal behaviour of floating marine litter released by rivers within the south-eastern Bay of Biscay based on riverine litter characterizations, drifters, and high-frequency radar observations and Lagrangian simulations. Virtual particles were released in the coastal area as a proxy of the floating fraction of riverine litter entering from rivers and reaching the open waters. Particles were parameterized with a wind drag coefficient (C_d) to represent their trajectories and fate according to the buoyancy of the litter items. They were forced with numerical winds and measured currents provided by high-frequency radars covering selected seasonal week-long periods between 2009 and 2021. To gain a better insight into the type and buoyancy of the items, samples collected from a barrier placed at the Deba River (Spain) were characterized at the laboratory. Items were grouped into two categories: low-buoyancy items (objects not exposed to wind forcing, e.g. plastic bags) and highly buoyant items (objects highly exposed to wind forcing, e.g. bottles). Overall, low-buoyancy items encompassed almost 90 % by number and 68 % by weight. Weakly buoyant items were parameterized with $C_\mathrm{d} = 0\,\%$ and highly buoyant items with $C_\mathrm{d} = 4\,\%$; this latter value is the result of the joint analysis of modelled and observed trajectories of four satellite drifting buoys released at the Adour (France), Deba (Spain), and Oria (Spain) river mouths. Particles parameterized with $C_\mathrm{d} = 4\,\%$ drifted faster towards the coast through the wind, notably during the first 24 h. In summer, over 97 % of particles beached after 1 week of simulation. In autumn this value fell to 54 %. In contrast, low-buoyancy items took longer to arrive at the shoreline, particularly during spring with fewer than 25 % of particles beached by the end of the simulations. The highest concentrations (> 200 particles km^{-1}) were recorded during summer for $C_\mathrm{d} = 4\,\%$ in the French region of Pyrénées-Atlantiques. Results showed that the regions in the study area were highly affected by rivers within or nearby the region itself. These results couple observations and a river-by-river modelling approach and can assist decision-makers on setting emergency responses to high fluxes of floating riverine litter and on defining future monitoring strategies for heavily polluted regions within the south-eastern Bay of Biscay.

1 Introduction

Rivers act as key vectors bringing improperly disposed and mismanaged litter from land into the marine environment. Riverine litter poses a large threat to freshwater systems by degrading aquatic life, impacting freshwater quality, and increasing economic losses linked with human activities (van Emmerik and Schwarz, 2020; Al-Zawaidah et al., 2021). However, most of the litter research conducted to date has focused on marine environments (87 %) when compared to freshwaters systems (13 %) (Blettler et al., 2018). Indeed, riverine litter contributions to oceans are still uncertain, and results vary depending on the input data and the model applied (Lebreton et al., 2017; Schmidt et al., 2017; Mai et al., 2020). Recent findings derived from extensive modelling efforts suggest that about 1600 rivers worldwide account for 80 % of plastic inputs to the ocean, with small urban rivers among the most polluting (Meijer et al., 2021). Mod-

Published by Copernicus Publications on behalf of the European Geosciences Union.

els require comprehensive field data and consistent and harmonized protocols to validate the amounts, type, and size of riverine inputs (González-Fernández and Hanke, 2017; Wendt-Potthoff et al., 2020; Margenat et al., 2021). Such comprehensive data were obtained in Europe thanks to the RIMMEL project (González-Fernández and Hanke, 2017). This research concluded that between 307 and 925 million floating riverine litter items are annually transferred into the ocean mainly through small rivers, streams, and coastal runoff (González-Fernández et al., 2021).

Once it has reached the sea, floating riverine litter can accumulate close to the shoreline or it can be transported to open waters, reaching even remote areas far from the coast. Indeed, the distribution and fate of floating litter in the marine environment is affected by the metocean conditions (currents, turbulence, wind) but also by the buoyancy of the objects (Ryan, 2015; Lebreton et al., 2019; Maclean et al., 2021). Objects with low buoyancy are mainly driven by currents, by contrast with highly buoyant items, which are driven along the water surface partially by winds. This wind effect ("windage") on floating marine litter behaviour has been further investigated by Lagrangian modelling studies in the open ocean (Allshouse et al., 2017; Maximenko et al., 2018; Lebreton et al., 2019; Abascal et al., 2009) when compared to the coastal area (Critchell and Lambrechts, 2016; van Utenhove, 2019; Tong et al., 2021). The lack of observational data is one of the key limitations for parameterizing the windage effect and accurately predict floating marine litter behaviour. However, observations derived from drifting buoys, such as those provided for decades by the Global Drifter programme, have been used to fill this gap. They have allowed simulating more realistic floating marine litter pathways from origin to fate by integrating experimental windage parameterizations and the corresponding comparison between observed and modelled trajectories (Duhec et al., 2015; Pereiro et al., 2018; Rizal et al., 2021). Nowadays, more affordable and environmentally friendly solutions are gaining force among researchers, as drifters are built using biopolymers (Novelli et al., 2017; D'Asaro et al., 2020) or have compact and lightweight designs with a GPS-tracking component for easy deployment (Meyerjürgens et al., 2019; van Sebille et al., 2021).

At the coastal scale, windage parameterization combined with realistic knowledge on coastal circulation becomes crucial to reduce the uncertainties of modelled trajectories (Van Sebille et al., 2020). Land-based high-frequency radar systems (hereafter HF radars, Rubio et al., 2017) offer the opportunity to monitor surface currents in coastal areas, where the transport processes are significantly more complex than in open-ocean waters due to the effect of the coast, the bathymetry, and other local forcings (e.g. river discharges or coastal upwellings). In the south-eastern Bay of Biscay (hereafter SE Bay of Biscay), as part of the operational oceanography system EuskOOS, an HF radar provides near-real-time surface currents fields. The system has already been used to study surface coastal transport processes in the area in combination with multisource data (Manso-Narvarte et al., 2018, 2021; Rubio et al., 2011, 2013, 2018, 2020; Solabarrieta et al., 2014, 2015, 2016). The HF radar is also a good example of effective monitoring of surface currents with strong potential for floating marine litter management. Research conducted by Declerck et al. (2019) in the SE Bay of Biscay provided the first assessment of floating marine litter transport and distribution in the region, coupling surface current observations from the EuskOOS system, Lagrangian modelling, and riverine inputs. Nowadays, these observations are used by local authorities both in real time and in hindcast in the framework of the operational service FML-TRACK to collect floating marine litter in the area. However, the accurate modelling of the transport and fate of floating marine litter needs to consider the variety of floating objects and sources and additional physical parameterization, such as windage.

This paper aims at estimating the seasonal behaviour of the floating marine litter fraction released by rivers within the SE Bay of Biscay reaching open waters. To do so, a Lagrangian model was forced by real observations from the EuskOOS HF radar and particles were parameterized to represent floating marine litter trajectories of two groups of items according to their buoyancy. Riverine litter collected from a local barrier was characterized at the laboratory to explore the fraction of high- and low-buoyancy items. Since most of the items were low-buoyancy, simulations considering only surface currents were performed as the reference. Complementary Lagrangian simulations for highly buoyant items (and less abundant in the area) were also performed. In this case, four low-cost buoys with a similar buoyancy to certain highly buoyant items were built and released in three different rivers. Drifter data were used to parameterize the wind effect on this type of item and consequently achieve more accurate results.

2 Study area

The study was conducted in the SE Bay of Biscay, between north-eastern Spain (Basque Country) and south-western France (Landes). The study area extends from 43.27 to 44.58° N and from 3.18 to 1.27° W, falling within the coverage area of the HF radar station of the operational oceanography system EuskOOS (Fig. 1). The study area comprises two Basque regions (Bizkaia (Spain) and Gipuzkoa (Spain)), two French departments (Pyrénées-Atlantiques and Landes), and eight rivers (Deba (Spain), Urola (Spain), Oria (Spain), Urumea (Spain), Oiartzun (Spain), Bidasoa (Spain), Nivelle (France), and Adour (France)). The mean annual river discharge varies widely between rivers from $3.71\,m^3\,s^{-1}$ (Oiartzun) to $350\,m^3\,s^{-1}$ (Adour) (Sheppard, 2018), and the population density differs between the Spanish and French border: 44.8 inhabitants km^{-2} (Landes) to

303.7 inhabitants km^{-2} (Basque Country) (Eurostat, 2019). The bathymetry in the SE Bay of Biscay is characterized by the presence of a narrow continental shelf ranging 7 and 24 km wide in the Basque area, gradually increasing along the French coast up to about 70 km (Bourillet et al., 2006; Rodríguez et al., 2021). The continental shelf in the SE Bay of Biscay comprises two main areas: the Aquitaine shelf with a N–S orientation and the Cantabrian shelf with an E–W orientation. The continental slope is very pronounced, with a slope of the order of 10 %–12 % (Sheppard, 2018). Over the continental shelf, the ocean circulation is marked by seasonal variability. At shorter temporal scales, circulation in the study area is mostly modulated by the bathymetry and the coastal orientation, the density-driven currents, and winds (Le Boyer et al., 2013; Solabarrieta et al., 2014). Tidal currents are quite weakly constrained by the topography and the width of the continental shelf (Lavin et al., 2006; González et al., 2007; Karagiorgos et al., 2020). Along-shelf currents are more intense and persistent during winter and autumn (about 10–15 $cm\,s^{-1}$), contrary to the other seasons, especially in summer (about 2.5 $cm\,s^{-1}$) (Charria et al., 2013). In winter, the prevailing SW winds causes an E to N flow from the Spanish coasts towards the French coasts. The moderate to strong NW winds occurring in spring and summer induce a S and SW surface current circulation accompanied by a greater variability (Solabarrieta et al., 2015). In winter, westerly winds in the Basque coast reinforce the slope current (named the Iberian Poleward Current (IPC)), a warm and saline intrusion trapped within 50 km of the shelf edge, reaching its greatest velocities (up to 70 $cm\,s^{-1}$) during this season. The IPC favours the along-slope transport of water masses (Solabarrieta et al., 2014; Porter et al., 2016). The exchange between shelf and deep-sea waters in winter is associated with the generation of eddies, from the interaction of currents with the topography (Lavin et al., 2006; Rubio et al., 2018; Teles-Machado et al., 2016). Maximum run-offs combined with SW winds also allow river plumes to spread northwards and along the French shore during winter. However, this path changes in spring, when river discharges are reduced and winds blow from the north-west (Lavin et al., 2006; Puillat et al., 2006).

First global modelling studies coupling ocean circulation and Lagrangian particle-tracking models reported that the SE Bay of Biscay is a hotspot for floating marine litter (Lebreton et al., 2012; van Sebille et al., 2012). Recent Lagrangian modelling studies combining measured and predicted surface currents by the HF radar and the Iberian Biscay Irish System (IBI) Copernicus model revealed that floating marine litter circulation in the SE Bay of Biscay is marked by a high seasonal variability. Results showed a higher retention during spring and summer and a northward dispersion along the French coast during autumn and winter (Declerck et al., 2019; Rubio et al., 2020). Surface currents derived from the Regional Ocean Modelling System (ROMS) and a particle-tracking model were combined by Pereiro et al. (2019) to track the numerical drifters representing floating marine litter in the Bay of Biscay. In this study, longer residence times and higher concentrations were observed in the SE Bay of Biscay when compared to north-western Iberian coastal waters, particularly in winter. From numerical simulations run using the HYCOM model, Rodríguez-Díaz et al. (2020) showed that floating marine litter items with high windage ($C_d = 3\,\%$–$5\,\%$) tend to accumulate in nearshore areas of the Bay of Biscay or end up beached. This trend is consistent with recent numerical simulations combining surface currents from the operational IBI and the numerical model TESEO that also revealed that the highly buoyant items ($C_d = 4\,\%$) rapidly beach in the SE Bay of Biscay, mainly in spring and summer (Ruiz et al., 2022a). Since June 2020, innovative detection and tracking solutions combining ocean modelling and remote observation systems have been operating in the SE Bay of Biscay to support floating marine litter reduction strategies both downstream (interception at the sea with collection vessels and on beaches with cleaning facilities) and upstream (source identification and reduction) (Delpey et al., 2021). However, research on floating marine litter behaviour in the SE Bay of Biscay is still in its early stage. Further experiments are needed to fully understand the role of windage, waves, and tides in the complex 3D circulation patterns governing coastal accumulation.

3 Methods and data

3.1 Riverine litter sampling

In spring 2018, a riverine barrier was placed in the Deba River (Gipuzkoa) to retain and collect floating riverine litter during low to moderate flows. This barrier enabled a passive sampling to characterize litter items in the lab. The barrier, which consisted of a nylon artisanal net supported by hard floats (buoys), was 40 m long and 0.6 m high with a 60 mm mesh size (see photos in Appendix A). The sampling was conducted weekly from April to June 2018. In total eight riverine litter samples were collected. Litter items were quantified, weighed, and categorized in the lab according to the master list included in the *Guidance on Monitoring of Marine Litter in European Seas* (Joint Research Centre, 2014). Items were grouped into seven types of material (artificial polymer materials, rubber, cloth/textile, processed/-worked wood, paper/cardboard, metal, and glass/ceramics) and further classified into 44 categories (see the classification in Appendix B). Riverine litter items were also categorized into two groups (low- and high-buoyancy items) considering their exposure to wind based on Ruiz et al. (2022a).

3.2 Drifter observations

Four satellite drifting buoys (herein after "low-cost buoys") were built by the authors and deployed one by one in the river mouths of the Deba (Buoy A), Oria (Buoy B), and Adour

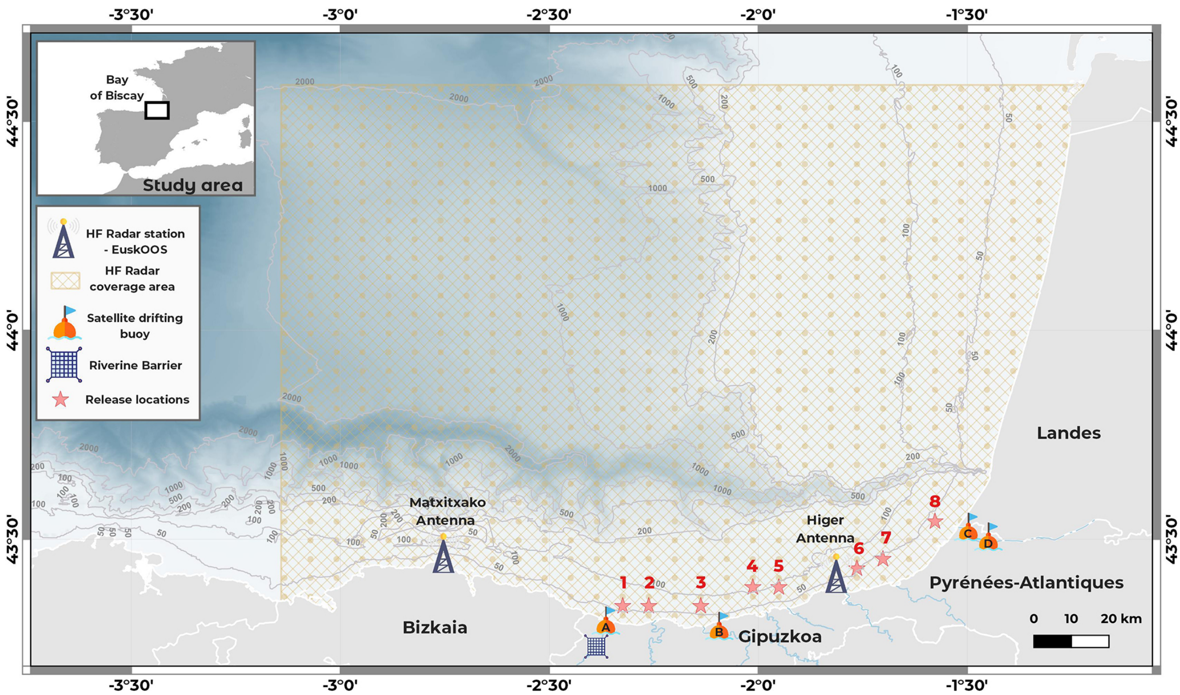

Figure 1. Study area with the release locations of the satellite drifting buoys and the riverine barrier. Dots in light yellow represent the nodes of the HF radar grid. Dots in orange represent the trajectories of the buoys. Numbers with stars in pink correspond to the particle releasing location for floating marine litter simulations: (1) Deba, (2) Urola, (3) Oria, (4) Urumea, (5) Oiartzun, (6) Bidasoa, (7) Nivelle, and (8) Adour rivers.

(buoys C and D) between April 2018 and November 2018 (Fig. 1, Table 1). The low-cost buoys provided positioning every 5 min using satellite technology. Low-cost buoys were 9 cm in height and 9.5 cm in float diameter and weighed approximately 200 g (Fig. 2). A GPS (SPOT Trace device) powered by four AAA cells was placed in the bottom of a high-density polyethylene (HDPE) plastic container sealed to guarantee water tightness. They were chosen because of their capability to ensure a reasonable balance between an accurate signal emission and their purchase and communication fees. SPOT Trace devices have been used over the past few years in coastal and open-ocean applications in a wide range of studies. Studies range from calibrating HF radars (Martínez Fernández et al., 2021) and tracking drifting objects such as icebergs (Carlson et al., 2020), pelagic *Sargassum* (Putman et al., 2020; van Sebille et al., 2021), or fishing vessels (Widyatmoko et al., 2021; Hoenner et al., 2022) to search and rescue training (Russell, 2017) and oil spill and litter monitoring (Novelli et al., 2018; Meyerjürgens et al., 2019). Almost two-thirds of the buoy floated above the water surface, thus preventing any satellite signal losses. Buoys A and D and transmitted their positions on an ongoing basis until their landing. Buoys B and C stopped emitting while they were drifting. In all cases, battery lifetime was enough for an adequate performance of the buoys. Once on land, citizens collected the buoys and reported their corresponding location.

3.3 HF radar current observations and wind data

Surface velocity current fields were obtained from the EuskOOS HF radar station composed by two antennas located at Matxitxako and Cape Higer and covering the SE Bay of Biscay since 2009, a range up to 150 km from the coast. The EuskOOS HF radar is part of JERICO-RI and it is operated following JERICO-S3 project best practices, standards, and recommendations (see Solabarrieta et al., 2016; Rubio et al., 2018, for details). Data consist of hourly current fields with a 5 km spatial resolution obtained from using the gap-filling OMA methodology (Kaplan and Lekien, 2007; Solabarrieta et al., 2021). In total, 85 OMA modes, built setting a minimum spatial scale of 20 km and applied to periods with data from the two antennas, were used to provide maximum spatiotemporal continuity in the HF radar current fields, which is a prerequisite of performing accurate Lagrangian simulations. The application of the OMA methodology has been validated for the Lagrangian assessment of coastal ocean dynamics in the study area by Hernández-Carrasco et al. (2018). HF radar velocities were quality controlled using procedures based on velocity and variance thresholds, signal-to-noise ratios, and radial and total coverage, following standard recommendations (Mantovani et al., 2020). Data subsets were built for the Lagrangian simulations avoiding periods with temporal gaps (still present in the case of the failure of one or two antennas) of more than a few hours. Hourly

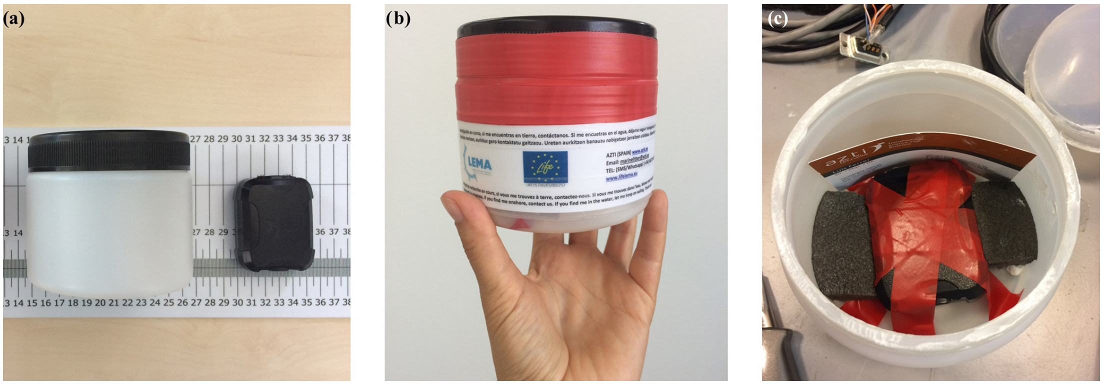

Figure 2. Main components of the low-cost buoy. The structure: **(a)** HDPE container and SPOT Trace device powered by four AAA cells. Assembly process: **(b)** final appearance once the buoy is sealed; the buoy is labelled with contact information both within and outside; **(c)** the SPOT Trace was fixed at the base of the container with adhesive tape to avoid twists and turns of the buoy.

Table 1. Locations, periods, and distances covered by the drifting buoys.

Buoy ID	River	Initial date (UTC+1)	Final date	Distance covered (km)
A	Deba	16 September 2018 08:00	4 October 2018 07:00	116.1
B	Oria	12 April 2018 16:00	18 April 2018 12:00	118.72
C	Adour	29 July 2018 20:00	2 August 2018 20:00	71.21
D	Adour	28 November 2018 09:00	30 November 2018 11:00	64.41

ERA5-U10-wind fields were obtained from the atmospheric reanalysis computed using the IFS model of the European Center for Medium-Range Weather Forecast (ECMWF) (see C3S, 2019 for details). The ERA5 atmospheric database covers the Earth on a 30 km horizontal grid using 137 vertical levels from the surface up to a height of 80 km and provides estimates of a large number of atmospheric, land, and oceanic climate variables, currently from 1979 to within 3 months of real time. Both HF radar current observations and wind data cover the drifter's emission periods and the selected week-long periods between 2009 and 2021 for riverine litter simulations (see Appendix C for the selected periods).

3.4 Particle transport model

The application of the transport module of the TESEO particle-tracking model (Abascal et al., 2007, 2017a, b; Chiri et al., 2020) was two-fold: (1) to simulate the transport and fate of floating marine litter entering from rivers and reaching the open waters of the SE Bay of Biscay and (2) to estimate a windage coefficient by calibrating the model according to the low-cost buoy trajectories. This module allows for simulating passive particles driven by surface currents, wind, and turbulent diffusion. Particle trajectories were calculated using the following equation:

$$\frac{\mathrm{d}\boldsymbol{x}i}{\mathrm{d}t} = \boldsymbol{u}_\mathrm{a}(\boldsymbol{x}_i, t) + \boldsymbol{u}_\mathrm{d}(\boldsymbol{x}_i, t), \tag{1}$$

where $\boldsymbol{u}_\mathrm{a}$ and $\boldsymbol{u}_\mathrm{d}$ are the advective velocity and diffusive velocity, respectively, for the $\boldsymbol{x}_i$ point and t time. The advective velocity is calculated as the lineal combination of the wind and currents according to

$$\boldsymbol{u}_\mathrm{a} = \boldsymbol{u}_\mathrm{c} + C_\mathrm{d}\boldsymbol{u}_\mathrm{w}, \tag{2}$$

where $\boldsymbol{u}_\mathrm{c}$ is the surface current velocity, $\boldsymbol{u}_\mathrm{w}$ is the wind velocity at 10 m over the sea surface, and C_d is the wind drag coefficient. The turbulent diffusive velocity is obtained using Monte Carlo sampling in the range of velocities $[-\boldsymbol{u}_\mathrm{d}, \boldsymbol{u}_\mathrm{d}]$, which are assumed to be proportional to the diffusion coefficients (Hunter et al., 1993; Maier-Reimer and Sündermann, 1982). For each time step Δt, the velocity fluctuation is defined as

$$|\boldsymbol{u}_\mathrm{d}| = \sqrt{\frac{6D}{\Delta t}}, \tag{3}$$

where D is the diffusion coefficient, whose value is $1\,\mathrm{m^2\,s^{-1}}$ in accordance with previously modelling work for floating marine litter (Pereiro et al., 2019; Ruiz et al., 2022a). Simulations were forced by HF radar surface current velocity and wind data and interpolated at the particle's position for integrating the trajectories. Beaching along the coast was implemented by a simple approach: if the particle reaches the shoreline, it is identified as beached, and it is removed from the computational process. TESEO has been calibrated and validated by comparing virtual particle trajectories to observed surface drifter trajectories at regional and local scale (Abascal et al., 2009, 2017a, b; Chiri et al., 2019). TESEO is a 3D numerical model conceived to simulate the transport and degradation of hydrocarbons, but it has also been successfully applied to the study of transport and accumulation of marine litter in estuaries (Mazarrasa et al., 2019; Núñez et al., 2019) and in open waters (Ruiz et al., 2022a).

3.4.1 Wind drag estimation

Two simulation strategies were combined for (1) estimating the wind drag coefficient and (2) studying the seasonal behaviour of floating items in the area (Sect. 3.5.2) The wind drag coefficient (C_d) was determined by comparing the observed trajectories provided by the low-cost buoys and the modelled trajectories performed with TESEO. The test was done through different parameterizations of the wind drag coefficient ranging from 0 % to 7 % (Table 2). This range was chosen based on previously floating marine litter studies coupling Lagrangian modelling and observations from satellite drifting buoys (Carson et al., 2013; Stanev et al., 2019; Van Der Mheen et al., 2019). The coefficient providing the lowest error was considered the best coefficient to simulate highly buoyant litter. Due to the grid limitations of the surface currents and wind data in the coastal area, the comparison was not initialized at the launching position of the low-cost buoys (river mouths), but instead it was initialized at the closest grid element that contained valid currents and wind data (Table 1). Observed positions were interpolated into a uniform 1 h time, fitting the metocean temporal resolution. A release of 1000 virtual particles was performed every 4 h at the corresponding observed position (Table 2). Particles were tracked over a 24 h period and the trajectory of the centre of mass of all the particles was computed at every time step to represent the track of the particle cloud. Observations were compared to modelled trajectories using the simple separation distance, which is the difference between the observed and the computed position of the centre of mass at a time step t. The mean separation distance $\overline{D(t^{\mathrm{mod}})}$ was calculated for every modelled position based on the simple separation distance following Eq. (4):

$$\overline{D(t^{\mathrm{mod}})} = \frac{1}{N}\sum_{i=1}^{N}\left|X^{\mathrm{mod}}\left(t^{\mathrm{mod}}\right) - X^{\mathrm{obs}}(t^{\mathrm{obs}})\right|, \tag{4}$$

where $X^{\mathrm{mod}}\left(t^{\mathrm{mod}}\right)$ and $X^{\mathrm{obs}}(t^{\mathrm{obs}})$ are the modelled and observed trajectories for the simulation period i of a total of N periods. A mean separation distance curve was computed for every wind drag coefficient derived from the mean separation distance curves of the four buoys. The area beneath the mean separation distance curve was calculated to select the more suitable wind drag coefficient. The area $\tilde{D}$ was calculated as a numerical integration over the forecast period via the trapezoidal method following Eq. (4). This method approximates the integration over an interval by breaking the area down into trapezoids with more easily computable areas:

$$\tilde{D} \approx \int_{t^{\mathrm{mod}=1}}^{t^{\mathrm{mod}=24}} \overline{D(t^{\mathrm{mod}})}\mathrm{d}t. \tag{5}$$

3.4.2 Lagrangian seasonal simulation of riverine litter items

Seasonal simulations were run for low- and high-buoyancy items to assess the seasonal differences in the transport and fate of floating riverine litter once it has reached the open waters of the SE Bay of Biscay. Particles were released around 2.5 nautical miles off the shoreline due to the complexity in resolving small-scale processes of floating riverine and marine litter behaviour in and close to the river mouths. As parameterizations concerning wind effect linked to the object characteristics are scarce, the optimal wind drag coefficient estimated for the buoys (see Sect. 3.5.1) was accounted for by simulating the behaviour of the objects highly exposed to wind. No wind drag parameterization ($C_\mathrm{d} = 0$ %) was applied for low-buoyancy objects not subjected to the wind effect. A total of 10 periods per season uniformly distributed within the study period (2009–2021) were considered for running the simulations based on the availability of HF radar surface current datasets (Appendix C). In total, 80 simulations (40 for $C_\mathrm{d} = 0$ % and 40 for $C_\mathrm{d} = 4$ %) were run for 7 d. For each simulation, 4000 particles were released in eight rivers (500 per river) assuming that river discharges are equal despite the seasonal variations and the morphological differences between rivers (Table 2). The total number of particles modelled for $C_\mathrm{d} = 0$ % was the same as $C_\mathrm{d} = 4$ %. Post-processing was carried out to compute by river (1) the particles' evolution over the time from their release until their arrival at the shoreline and (2) the particles' distribution on the shoreline, counting the number of beached particles per kilometre of shoreline and indicating the spatial concentration per region.

4 Results

4.1 Riverine litter characterization

In total 1576 items and 11.597 kg of floating riverine litter were sampled and characterized (Fig. 3). Plastic was the most common type of riverine litter in terms of the number of items (95.1 %) and in weight (67.9 %); they were also frequent glass/ceramics (16.1 %) and cloth/textile items (6.9 %) when counted by weight. The top 10 litter items accounted for 93.3 % by number and 72.6 % by weight of the total riverine litter (Table 3). Plastic/polystyrene pieces between 2.5 and 50 cm and other plastic/polystyrene identifiable items

Table 2. Simulation, release, and physical parameter values for wind drag estimation and floating riverine litter simulations.

	Simulation parameters			Release parameters		Physical parameters	
	Number of particles	Integration time	Time step	Release locations	Release time	Turbulent diffusion coefficient	Wind drag coefficient (C_d)
Simulations for wind drag estimation	1000 per location	24 h	60 s	At the observed locations of the buoy	Over the emitting period of the buoy at spaced intervals of 4 h	$1\,\mathrm{m^2\,s^{-1}}$	0 %, 2 %, 3 %, 4 %, 5 %, 6 %, 7 %
Seasonal riverine litter simulations	500 per river	1 week	60 s	At a distance of 2.5 nautical miles from the river mouth	At the beginning of the selected time period (10 periods per season)	$1\,\mathrm{m^2\,s^{-1}}$	0 %, 4 %

(e.g. food labelling) were the most abundant in terms of number (71.2 %) and weight (16.9 %). Weakly buoyant items encompassed almost 91 % by number and 68 % by weight of litter items (Fig. 4).

4.2 Wind drag coefficient for drifting buoys

Total distances covered by drifting buoys ranged from 62 to 118 km (Table 1), and they all scattered over the HF radar coverage area. Buoys provided their position data over 385 h before beaching on the Landes and Gipuzkoa shorelines. When compared with numerical trajectories obtained using different C_d parameterizations, the mean separation distance ($\overline{D(t^{\mathrm{mod}})}$ increased nearly linearly with time for all the parameterizations, achieving a maximum separation of almost 14 km at 24 h for $C_\mathrm{d} = 0\,\%$ (Fig. 5). Overall, using no windage parameterization provided the largest $\overline{\widetilde{D}}$. Simulations parameterized with $C_\mathrm{d} = 4\,\%$ provided the best results with an average ± standard deviation (SD) of 3.2 ± 1.25 km and a maximum value of 4.85 km at 24 h. When assessing the mean separation distance for all the modelled positions at every observed position of the buoys, the most common range separation distance for $C_\mathrm{d} = 4\,\%$ was 2–4 km (Fig. 6). Hence, a wind drag coefficient of 4 % was applied in the remaining analysis to estimate the behaviour of highly buoyant items.

4.3 Seasonal trends in floating riverine litter transport and fate

Particle concentration on the shoreline varied between 0 and 258.46 particles km^{-1} (Fig. 7). Particles parameterized with $C_\mathrm{d} = 4\,\%$ drifted faster towards the coast, notably during the first 24 h. The highest concentrations (> 200 particles km^{-1}) were recorded during summer in Pyrénées-Atlantiques for $C_\mathrm{d} = 4\,\%$, probably due to the seasonal retention patterns within the study area (Appendix D). Although less intensely, $C_\mathrm{d} = 4\,\%$ also led to a high particle concentration in Pyrénées-Atlantiques (106.86 particles km^{-1}) and Gipuzkoa (166.1 particles km^{-1}) during winter. The lowest concentrations (0–20 particles km^{-1}) were recorded for $C_\mathrm{d} = 0\,\%$ after the first 24 h of simulation, particularly during autumn. Overall, Bizkaia was the less impacted region for both windage coefficients (< 40 particles km^{-1}). During summer, over 97 % of particles parameterized with $C_\mathrm{d} = 4\,\%$ beached after 1 week of simulation (Fig. 8). In autumn this value fell to 54 %. In contrast, beached particles parameterized with $C_\mathrm{d} = 0\,\%$ were less abundant by the end of the simulations, particularly during spring with less than 25 % of particles trapped in the shoreline.

Overall, the average of particles parameterized with $C_\mathrm{d} = 0\,\%$ was higher when comparing to $C_\mathrm{d} = 4\,\%$ (Fig. 9). Particles released in French rivers and parameterized with $C_\mathrm{d} = 0\,\%$ were less abundant during summer, though this trend was reversed in autumn. For $C_\mathrm{d} = 0\,\%$, the number of particles released in the Bidasoa River during summer were the least abundant after 1 week of simulation (< 200 particles on average). The vast majority of particles released in the Urumea River during winter were floating in the study area by the end of the simulations (479 particles on average). Particles parameterized with $C_\mathrm{d} = 4\,\%$ beached faster during the first 48 h, mainly in summer and for those particles released in the French rivers. During this season, the average number of particles floating in the study area by the end of the simulation ranged between 0 and 250. Similar trends were observed within the same season between rivers, probably influenced by the vicinity of rivers and the spatiotemporal resolution of forcings. Over 40 % of the total particles parameterized with $C_\mathrm{d} = 4\,\%$ and almost 12 % parameterized with $C_\mathrm{d} = 0\,\%$ beached in Gipuzkoa (Fig. 10). During spring, almost 60 % of beached particles parameterized with $C_\mathrm{d} = 0\,\%$ were located Bizkaia. For $C_\mathrm{d} = 0\,\%$, particles released during summer in the rivers located in the western area of Gipuzkoa drifted longer distances and reached the Landes shoreline. This trend changed during winter, when the vast majority of particles released in Gipuzkoa rivers beached mainly in

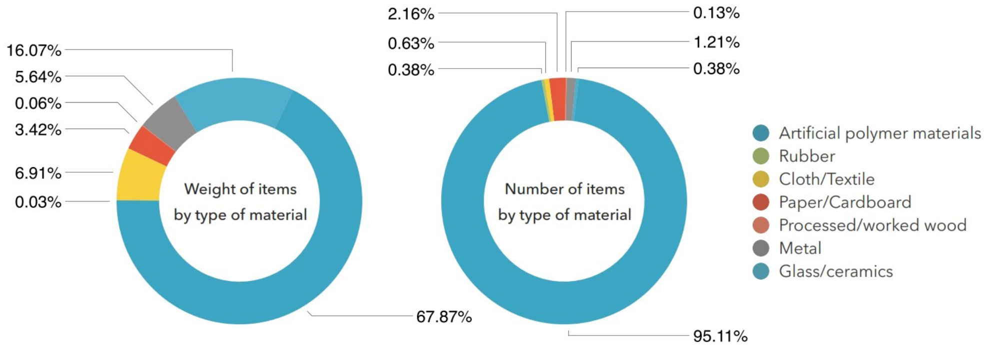

Figure 3. Composition of riverine litter by type of material in terms of the number of items and weight. Items were collected by the barrier placed in the Deba River (Gipuzkoa) between April and June 2018.

Table 3. Top 10 (X) riverine litter items collected from the barrier located in the Deba River (Gipuzkoa) between April and June 2018. Items have been ranked by abundance (left) and weight (right) according to the master list categories of beach litter items and classified based on their exposure to the wind effect.

Top X by number of items				
Ranking	TSG_ML General code	General name	Number of items (%)	Type of item
1	G76	Plastic/polystyrene pieces 2.5 cm >< 50 cm	71.19%	Low buoyant
2	G10	Food containers incl. Fast food containers	6.21%	Highly buoyant
3	G124	Other plastic/polystyrene items (identifiables)	3.68%	Low buoyant
4	G30	Crips packets/sweet wrappers	3.55%	Low buoyant
5	G20-G24	Plastic caps and lids/Plastic rings	2.41%	Low buoyant
6	G96	Sanitary towels/panty liners/ backing strips	2.22%	Low buoyant
7	G158	Other paper items	1.33%	Low buoyant
8	G5	What remains of rip-off plastic bags	1.33%	Low buoyant
9	G77	Plastic/polystyrene pieces >50 cm	0.82%	Low buoyant
10	G3	Shopping bags incl.pieces	0.51%	Low buoyant
		TOTAL	93.25%	

Top X by weight of items				
Ranking	TSG_ML General code	General name	Weight (%)	Type of item
1	G124	Other plastic/polystyrene items (identifiables)	16.88%	Low buoyant
2	G200	Bottles incl. Pieces	15.80%	Highly buoyant
3	G76	Plastic/polystyrene pieces 2.5 cm >< 50 cm	9.48%	Low buoyant
4	G96	Sanitary towels/panty liners/backing strips	9.48%	Low buoyant
5	G10	Food containers incl. Fast food containers	6.04%	Highly buoyant
6	G135	Clothing (clothes, shoes)	4.16%	Low buoyant
7	G77	Plastic/polystyrene pieces > 50 cm	2.91%	Low buoyant
8	G145	Other textiles (incl.rags)	2.77%	Low buoyant
9	G175-G176	Cans (beverage/food)	2.60%	Highly buoyant
10	G3	Shopping bags incl.pieces	2.52%	Low buoyant
		TOTAL	72.64%	

Gipuzkoa and Bizkaia. Beached particles parameterized with $C_d = 0\,\%$ experienced more seasonal variations derived from the surface current circulation patterns within the SE Bay of Biscay. For $C_d = 4\,\%$, particles beached in Gipuzkoa ranged between 51 % in spring and 38 % in winter, and Bizkaia was the less affected region despite the season. Overall, all regions were highly affected by rivers within or nearby the region itself.

5 Discussion

5.1 Riverine litter composition

An artisanal net placed at the mouth of the Deba River enabled sampling riverine litter in the study area during spring 2018. Short and narrow rivers prevail in the SE Bay of Biscay, affected by a strong tidal regime and very intense, stationary and persistent storms (Ocio et al., 2015). Studies aiming at reporting the abundance and composition of floating riverine litter in European rivers date back less than 10 years, and they were performed in larger and more abundant rivers than the Deba River. Despite the morphology and hydrological differences, plastic was the predominant material in the Deba River, as in the Siene (Gasperi et al., 2014), Danube (Lechner et al., 2014) or Rhine River (van der Wal et al., 2015). Similarities were also found when comparing the top 10 list of riverine litter items to rivers located in the north-east Atlantic region. Plastic/polystyrene pieces between 2.5 and 50 cm (71.2 %) top the list in terms of the number of items, and their abundance was slightly higher when compared to north-east Atlantic rivers (54.53 %) (Bruge et al., 2018; González-Fernández et al., 2018). Lower abundances were observed in the Mediterranean (25.01 %) and the Black Sea (13.74 %). Riverine litter items trapped on vegetation or deposited on the riverbank can be degraded by weather conditions (rain, wind, etc.) favouring the fragmentation in plastic pieces before their arrival in the coastal and marine environment (Chamas et al., 2020). The fragmentation can be also influenced by the material and the shape of the litter

FLOATING RIVERINE LITTER CLASSIFICATION BY WIND EXPOSURE

	Highly buoyant items	Low buoyant items
Number of items	1,436	140
Weight of items (kg)	7.880	3.717

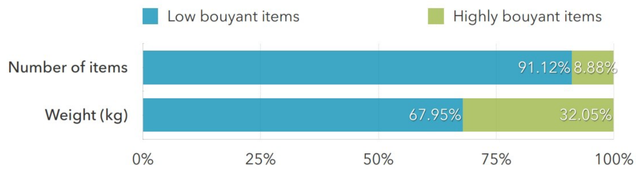

Figure 4. Riverine litter classification based on the exposure to the wind effect. Items were collected from the barrier located in the Deba River (Gipuzkoa) between April and June 2018.

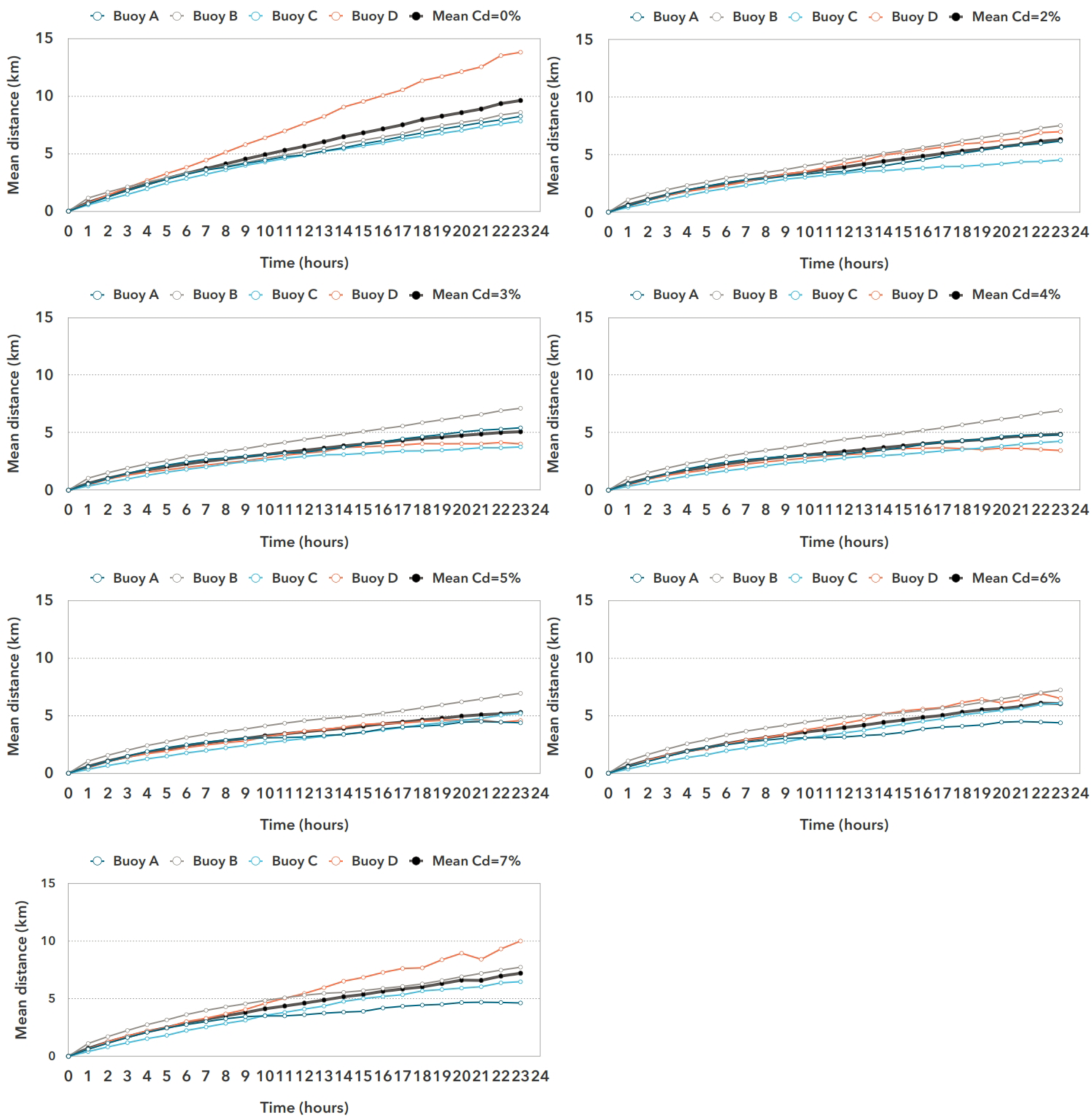

Figure 5. Mean separation distance between modelled and observed trajectories for each wind drag coefficient. The dark line is the mean curve used for the trapezoidal integration.

items (Woods et al., 2021). Differences in plastic/polystyrene pieces between 2.5 and 50 cm abundances can be attributed to a faster fragmentation due to the variations in weather conditions between river basins. However, more detailed analyses on the physical characteristics of litter items (i.e. polymer type) are necessary to fully assess their impact on the occurrence of fragmented plastic pieces. Results are also in line with the ranking list of the top 10 beach litter items across the north-east Atlantic region revealing that single-use plastics (i.e. food containers, bottles, and other packaging) are among

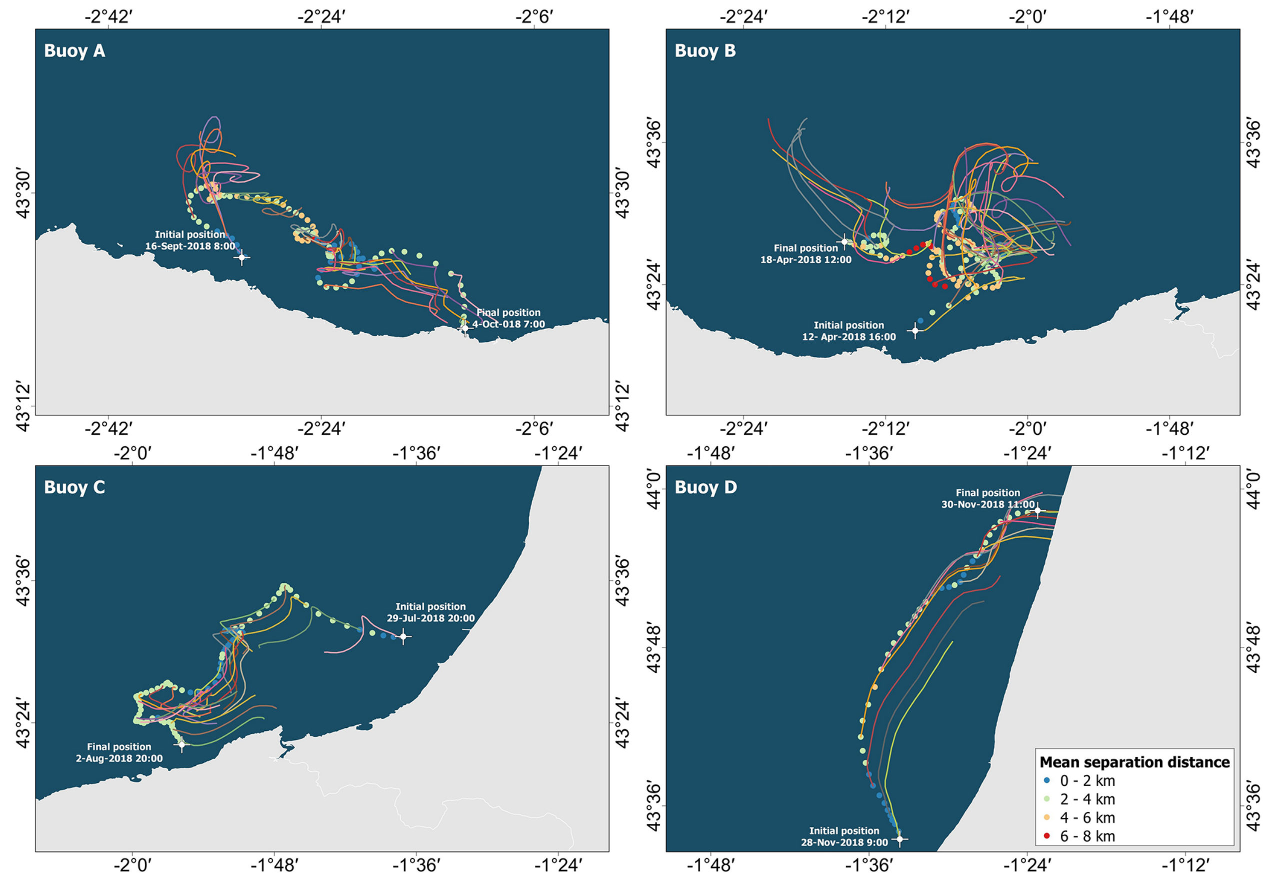

Figure 6. Spatial mean distance between modelled and observed trajectories of buoy A, B, C, and D with a drag coefficient $C_d = 4\,\%$. Particle trajectories were simulated during 24 h, with a re-initialization period every 4 h. The modelled trajectories are shown in solid lines. Circles represent the mean separation distance at the observed position for all the modelled positions.

the most abundant riverine litter items together with plastic fragments (European Commission, 2018). These results differed from the analysis performed in sea small-scale convergence areas of floating marine litter ("litter windrows") on the coastal waters of the SE Bay of Biscay, where fishing-related items were the second most abundant sub-category in terms of number after plastic/polystyrene pieces between 2.5 and 50 cm (Ruiz et al., 2020). Substantial differences also exist between riverine litter sampled in the Deba River and floating marine litter assessed by visual observation from research vessels in open waters of the Bay of Biscay (Ruiz et al., 2022a). Differences might be related to the monitoring method and, also, to the size of the items, since small items, such as plastic pieces, can be overlooked by the observer when the visual counting method is applied, contrary to riverine litter samplings for later analysis in the lab. Overall, riverine litter data acquisition is mainly focused on the floating fraction, and the litter loads under the surface water are often ignored. Increasing the quantity of rivers sampled, the frequency, and the riverine water compartments is necessary to establish the composition and trends of riverine litter in the SE Bay of Biscay.

5.2 Wind drag estimation

One of the largest uncertainties for predicting floating riverine and marine litter behaviour is the proper quantification of a wind drag coefficient. Wind drag estimations conducted so far for floating marine litter items range between 0 % and 6 % (Ko et al., 2020; Critchell and Lambrechts, 2016; Neumann et al., 2014) with an upper limit of 10 % (Yoon et al., 2010). However, only a few of them have been validated using observational data (Maximenko et al., 2018; Callies et al., 2017). In this study, data provided by low-cost buoys combined with surface current measurements by HF radar were used as a proxy for modelling the drift of floating litter objects with similar buoy characteristics (density, size, and shape). Results demonstrated that $C_d = 4\,\%$ was the optimal wind drag coefficient for accurately represent the pathways of the low-cost buoys in the study area. This value can be consistent with the estimations of the partially emerged *Physalia physalis* for the Bay of Biscay (Ferrer and Pastor, 2017), but it is almost 3 times higher than the maximum wind drag coefficient reported in the area by Pereiro et al. (2018). This can be explained by the fact that buoys

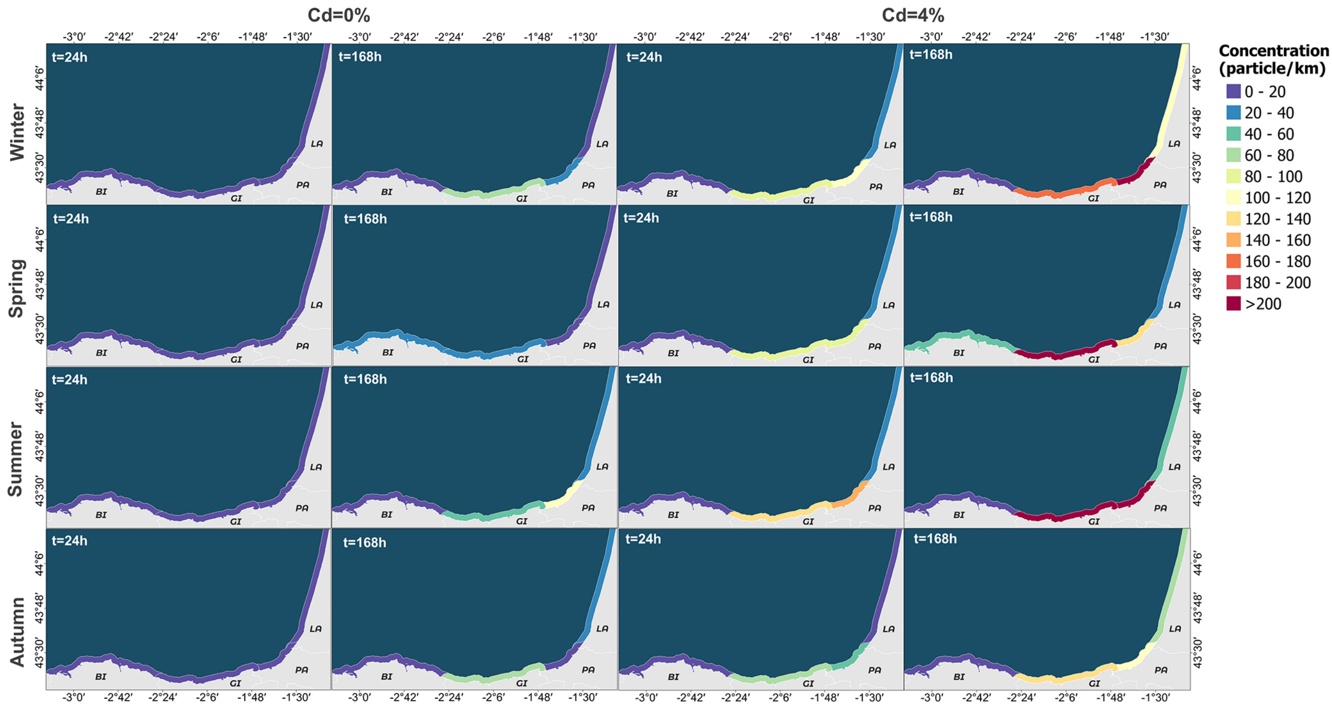

Figure 7. Particle concentration on the Bizkaia, Gipuzkoa, Pyrénées-Atlantiques, and Landes shoreline. The seasonal distribution is shown for $C_\mathrm{d} = 0\,\%$ and $C_\mathrm{d} = 4\,\%$ after 24 and 168 h of simulation.

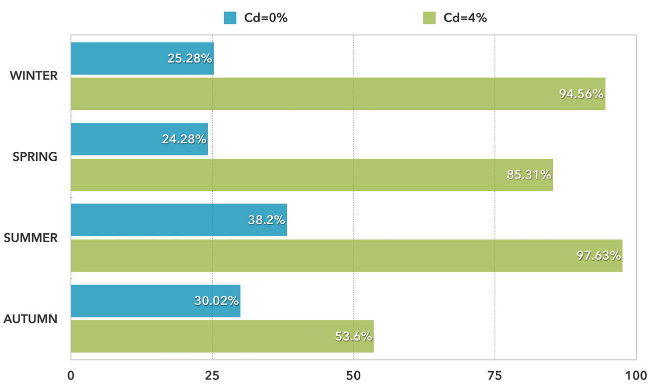

Figure 8. Seasonal numbers of beached particles parameterized with $C_\mathrm{d} = 0\,\%$ and $C_\mathrm{d} = 4\,\%$ after 168 h of simulation.

used in the experiment remained submerged beneath the sea surface and were less exposed to the wind effect. The estimated wind drag coefficient was also greater than $C_\mathrm{d} = 3\,\%$ observed for the Prestige oil spill accident (Abascal et al., 2009; Marta-Almeida et al., 2013). Indeed, oil spill studies refer to a range of wind drag coefficient between 2.5 % to 4.4 % of the wind speed, with a mean value of 3 %–3.5 % (e.g. ASCE, 1996; Reed et al., 1994). Object characteristics may change over time due to the exposure to wind, waves, UV radiation, seawater, and the attachment of organic material (Kooi et al., 2017; Min et al., 2020). Objects become breakable, and biofouling increases their density, overcoming the positive buoyancy and impacting their trajectory. Investigations so far pinpointed longer timescales (weeks to months and longer) than considered in this study (days) for a significant change on the behaviour of floating objects (Ryan, 2015; Fazey and Ryan, 2016). Consequently, physical variations in the buoy properties were not accounted for the wind drag estimation. The separation distance between observed and modelled trajectories has been commonly used to evaluate the skill of particle-tracking models (Callies et al., 2017; Haza et al., 2019; Aksamit et al., 2020; Abascal et al., 2012). In this study, the purpose was not to evaluate the model accuracy but to estimate the wind drag coefficient for the low-cost buoys. However, the novel approach proposed by Révelard et al. (2021) may be of particular interest for future experiments oriented towards assessing the wind drag coefficient of highly buoyant items drifting for short time periods in the coastal area.

5.3 Seasonal riverine litter distribution by region

It is broadly accepted that the SE Bay of Biscay is polluted with floating marine litter discarded or lost in the marine and coastal area but also with litter originating inland and transported via rivers and run-off. However, detailed studies on riverine litter contribution are still scarce, and modelling efforts combining observations and physical parameterizations of floating litter properties are non-existent. This study shows that the exposure to the wind effect largely controls the trans-

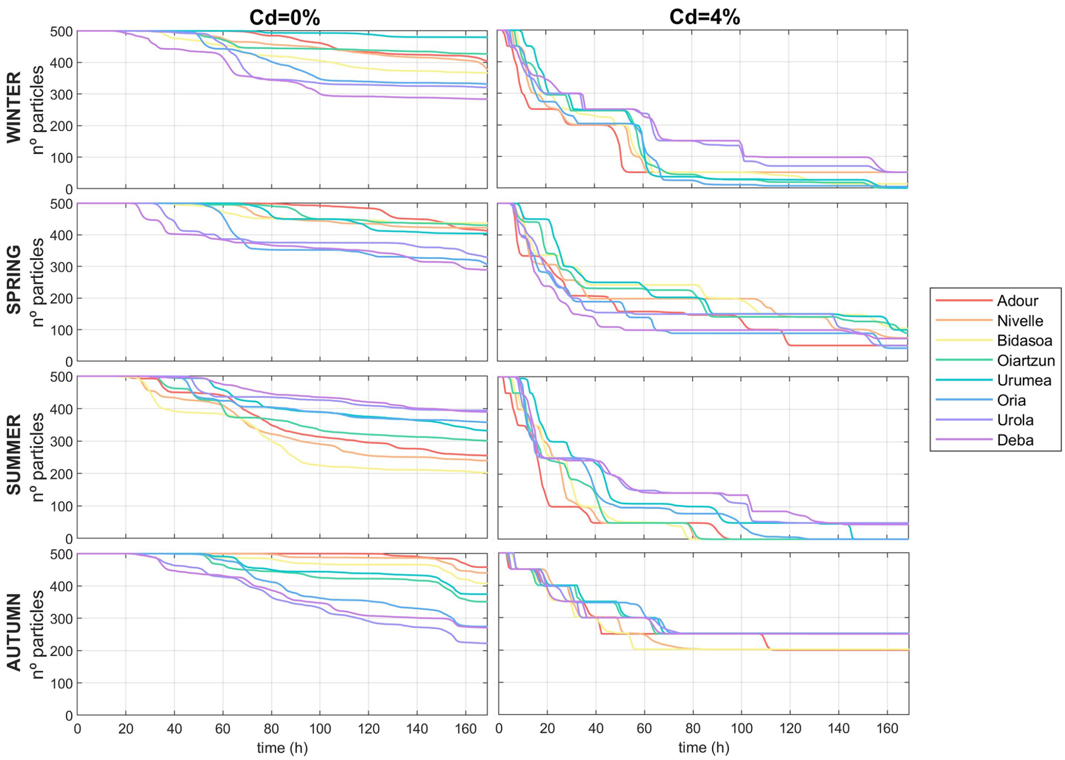

Figure 9. Temporal evolution of the particles parameterized with $C_d = 0\,\%$ and $C_d = 4\,\%$ throughout the different seasons. The curves represent the average number of particles floating in the water surface by river and for every time step.

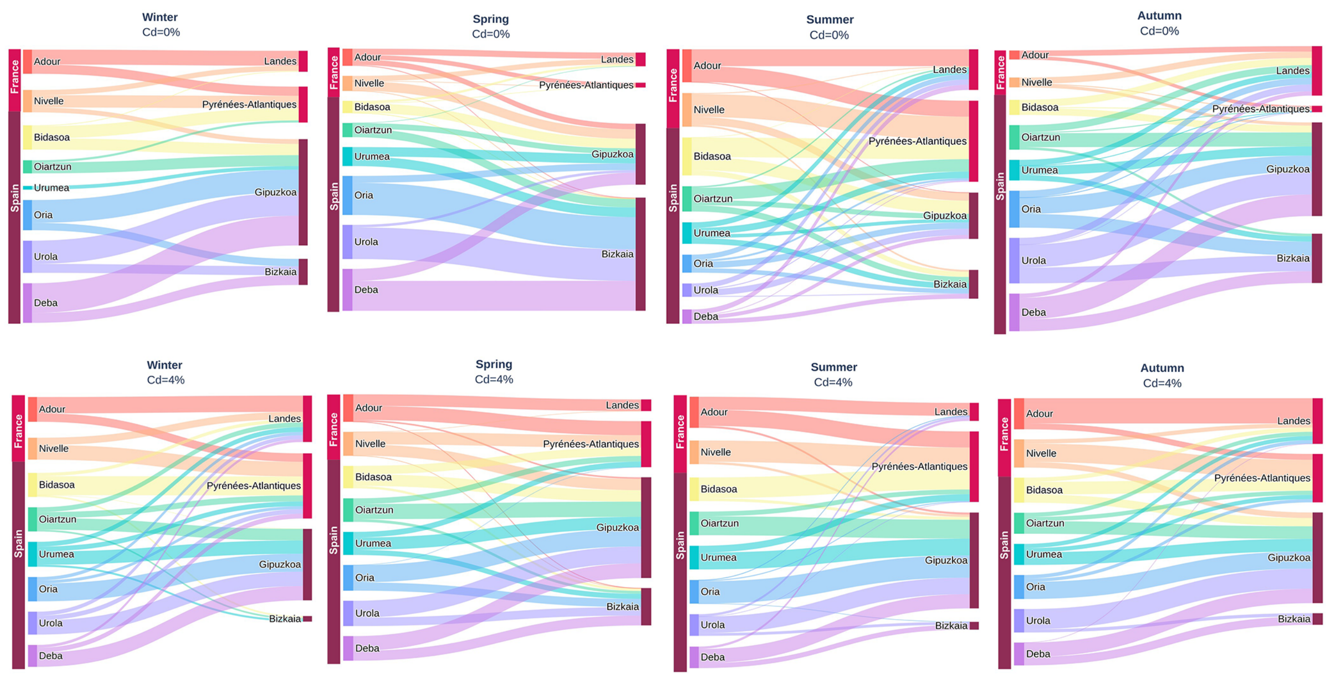

Figure 10. Seasonal analysis of the beached particles parameterized with $C_d = 0\,\%$ and $C_d = 4\,\%$ per region and river by the end of the simulation period. The nodes of the region correspond to the number of beached particles. The country to which each river belongs – France (Pyrénées-Atlantiques) and Spain (Gipuzkoa) – is shown on the left side of each figure. The width of the node depicts the sum of the beached particles, and the links represent the number of particles beached per river.

port and coastal accumulation of floating marine litter in the SE Bay of Biscay, with concentrations varying between regions and over time. Concentrations in Pyrénées-Atlantiques and Gipuzkoa differed widely from the other studied regions. Indeed, the highest concentrations occurred in both regions during summer for low- (100–120 particle km^{-1}) and high-buoyancy items (> 200 particles km^{-1}). A higher number of particles beached in Gipuzkoa during summer when compared to Pyrénées-Atlantiques, but concentrations were lower since the Basque shoreline is longer. The pathways and fate of low-buoyancy items reflect the seasonal surface water circulation patterns in the SE Bay of Biscay. Results are in line with findings provided by Declerck et al. (2019) who pinpointed a higher coastal retention in the area during spring and summer. Weakly buoyant objects remained floating at the coastal waters and highly buoyant objects tended to beach remarkably faster as reported in literature by Rodríguez-Díaz et al. (2020). However, long-term data collected by in situ observations of beached litter across the different regions are necessary to validate the large seasonal variations and to assess the reliability of concentration levels for addressing riverine litter issue in priority regions with heavily polluted coastlines.

5.4 Rivers as key vectors of riverine litter

The interpretation of the spatial and temporal riverine litter distribution by river can be challenging since riverine litter fluxes in the study area are highly uncertain. In the study area, two major assumptions were made regarding the river systems: (1) the same river discharge for all rivers and (2) the same river discharge for all seasons. This means that the same amounts of riverine litter were allocated for every river regardless of the differences in the width and depth and the seasonal flow variations. Since each river basin has its own particularities, future modelling approaches should be adapted to the morphology and hydrological conditions of the catchment area. Other drivers, such as the land use or population density, can be a determining factor for the amount of mismanaged litter that could contribute to riverine litter fluxes (Schmidt et al., 2017; Schuyler et al., 2021). It is also necessary to further investigate if higher river flows in the area are directly related to an increased discharge of riverine litter since analysis already performed in different river basins shows contradicting relations between the occurrence of riverine litter and river fluxes (van Emmerik and Schwarz, 2020). Along with the complex nature of qualifying riverine litter fluxes, litter behaviour in the coastal area of the SE Bay of Biscay is still in its early stage, and much has yet to be revealed. Particular attention should be paid to Pyrénées-Atlantiques and Gipuzkoa, as the main impacted regions in the studied area. Rivers in the study area are mainly located in Gipuzkoa, which favours the accumulation of floating litter in this region regardless of the season. Regional coordination should be reinforced due to the transboundary movement of floating riverine litter in the study area and reasonable efforts oriented towards retaining or removing riverine litter as clean-up measures in the riverbanks should be investigated to avoid litter being transported to the coastal and marine environment.

5.5 Model limitations

The interaction between floating litter and the shoreline is highly complex and relies on many processes including waves and tides. Indeed, waves and tides can constrain coastal accumulation since they can resuspend and transport litter back into the ocean (Brennan et al., 2018; Compa et al., 2022). The geomorphology can also affect the retention of litter washing ashore. Sandy beaches tend to be more efficient at trapping and accumulating litter than rocky areas, which favour litter fragmentation (Robbe et al., 2021; Weideman et al., 2020). How these processes contribute to the actual beaching is unknown, and they cannot be resolved yet at a suitable resolution (Melvin et al., 2021). In this study, particles were released in open waters, and once they reached the shoreline, they were classified as beached. The tidal effect and the wave-induced Stokes drift were not accounted for to avoid introducing more uncertainties. However, further field and laboratory experiments to better understand how these processes influence floating litter behaviour on the coastline are recommend. For future research, it is also important to consider exploring the effect of the type of shoreline on coastal accumulation. In this study, a constant diffusion coefficient of $1\,m^2\,s^{-1}$ was regarded as a pragmatic choice based on previous modelling work for floating marine litter. However, more field measurements are necessary to accurately assess the influence of the diffusion process on the transport of floating marine litter.

6 Conclusions

The SE Bay of Biscay has been described by global and regional models as an accumulation zone for floating marine litter. However, detailed studies on floating riverine litter behaviour once items arrive in open waters are still scarce. Based on HF radar current observations and a wind dataset, this contribution tries to fill this gap by providing insights into how low- and high-buoyancy litter released by several rivers of the SE Bay of Biscay may affect the nearby regions seasonally in terms of concentration and beaching. Analysis of riverine litter samples collected by a barrier placed in the study area showed that low-buoyancy objects were predominant, although highly buoyant objects were also relevant in terms of weight. Simulations for assessing the seasonal trends of floating riverine litter transport and fate were performed with the Lagrangian model TESEO. To properly integrate the differences in litter buoyancy, simulations were parameterized with a wind drag coefficient for low- and high-buoyancy items. The wind drag for highly buoyant items was estimated by comparing the observed and the modelled positions of four drifters. The developed low-cost buoys proved to be suitable to provide real-time trajectories of highly buoyant objects exposed to wind. However, drifters with different characteristics should be used in future studies to account for the windage effect on different types of items. The transport and fate of both high- and low-buoyancy items released by rivers was calculated by season. Highly buoyant items rapidly beached (in less than 48 h), particularly in summer and winter; in contrast, despite the season over two-thirds of low-buoyancy items remained floating after 1 week of being released. This highlights the discrepancy between the behaviour for low- and high-buoyancy objects and the importance of parameterizing the windage effect in order to accurately predict riverine litter accumulation in the coastal area of the SE Bay of Biscay. Beached particles were mainly found in Gipuzkoa regardless of the season and the wind drag coefficient. Overall, the less affected region was Bizkaia with the exception of a spring period for low-buoyancy items. Despite the season, most of the riverine litter remained in the study area and rivers polluted the regions within the river basin or surrounding it. Investigating what beaches are most likely to accumulate large quantities and the contribution per river can provide relevant input to response operations after storm events in the short to medium term and can also support the identification of priority rivers for a monitoring programme, assisting adapted intervention of riverine pollution regionally in the future.

Appendix A: Floating barrier for riverine litter collection

Figure A1. Floating barrier **(a)** and installation in the Deba River (Gipuzkoa) **(b)**.

Appendix B: Riverine litter classification based on the exposure to the wind effect

Table B1. Data were gathered from surveys carried out during spring 2018 in the Deba River (Gipuzkoa).

TSG_ML General code	General name	Number of items	Weight (kg)
Weakly buoyant items transported by currents			
G1	Four- or six-pack yokes, six-pack rings	1	3.3
G2	Bags	7	170.7
G3	Shopping bags incl. pieces	8	292.44
G4	Small plastic bags, e.g. freezer bags	4	50.9
G5	What remains from rip-off plastic bags	21	186.31
G20–G24	Plastic caps and lids/plastic rings	38	216.39
G26	Cigarette lighters	1	9.7
G27	Cigarette butts and filters	1	0.1
G30	Crisps packets/sweet wrappers	56	250.2
G31	Lolly sticks	1	2.4
G32	Toys and party poppers	2	97.5
G36	Fertilizers/animal feed bags	1	11.5
G48	Synthetic rope	2	6.7
G76	Plastic/polystyrene pieces 2.5 cm > < 50 cm	1122	1788.32
G77	Plastic/polystyrene > 50 cm	13	337.34
G96	Sanitary towels/panty liners/backing strips	35	1099.8
G100	Medical/pharmaceutical containers/tubes	7	69.4
G101	Dog faeces bags	2	106
G124	Other plastic/polystyrene items (identifiable)	58	1958.5
G125	Balloons and balloon sticks	5	1.1
G134	Other rubber pieces	1	1.6
G135	Clothing (clothes, shoes)	3	481.7
G145	Other textiles (incl. rags)	7	320.5
G148	Cardboard (boxes and fragments)	3	85.7
G156–G157	Paper and paper fragments	2	121.2
G158	Other paper items	4	69.1
G159	Corks	4	21.2
G173	Other (specify)	21	99.3
G177	Foil wrappers, aluminium foil	1	7
G179	Bottle caps, lids, and pull tabs	1	0
	Total	91.12 %	67.95 %
Highly buoyant items transported by wind and currents			
G7	Drink bottles <= 0.5 L	5	142.6
G8	Drink bottles > 0.5 L	3	91.1
G9	Cleaner bottles and containers	2	105.7
G10	Food containers incl. fast-food containers	98	723.9
G11–G12	Cosmetics bottles and other containers (shampoo, shower gel, deodorant)	4	100.3
G17	Injection gun containers	1	18.3
G33	Cups and cup lids	6	32.6
G150–G151	Cartons/Tetra Pak	2	121.2
G153	Cups, food trays, food wrappers, drink containers	4	69.1
G174	Aerosol/spray can industry	2	143.2
G175–G176	Bottle caps, lids, and pull tabs	2	5
G177	Bottles incl. pieces	5	1832.3
G178	Light bulbs	1	31.7
	Total	8.88 %	32.05 %

Appendix C: Selected seasonal week-long periods from the HF radar (2009–2021)

Table C1. Periods selected between 2009 and 2021 based on the availability surface current datasets provided by the HF radar.

Winter										
	Period 1	Period 2	Period 3	Period 4	Period 5	Period 6	Period 7	Period 8	Period 9	Period 10
Initial date	7 Feb 2013 08:00	9 Mar 2021 22:00	23 Jan 2009 01:00	2 Jan 2013 11:00	18 Jan 2016 17:00	2 Jan 2014 15:00	17 Feb 2017 06:00	17 Jan 2012 09:00	22 Jan 2017 17:00	12 Jan 2021 23:00
Final date	14 Feb 2013 07:00	16 Mar 2021 21:00	30 Jan 2009 00:00	9 Jan 2013 10:00	25 Jan 2016 16:00	9 Jan 2014 14:00	24 Feb 2017 05:00	24 Jan 2012 08:00	29 Jan 2017 16:00	19 Jan 2021 22:00
Spring										
	Period 1	Period 2	Period 3	Period 4	Period 5	Period 6	Period 7	Period 8	Period 9	Period 10
Initial date	14 Apr 2015 23:00	16 May 2012 00:00	16 Apr 2017 14:00	21 Apr 2012 08:00	5 Jun 2014 06:00	11 Apr 2021 20:00	6 May 2012 06:00	10 Apr 2015 08:00	8 May 2018 22:00	22 Apr 2016 11:00
Final date	21 Apr 2015 22:00	22 May 2012 23:00	23 Apr 2017 13:00	28 Apr 2012 07:00	12 Jun 2014 05:00	18 Apr 2021 19:00	13 May 2012 05:00	17 Apr 2015 07:00	15 May 2018 21:00	29 Apr 2016 10:00
Summer										
	Period 1	Period 2	Period 3	Period 4	Period 5	Period 6	Period 7	Period 8	Period 9	Period 10
Initial date	19 Aug 2017 01:00	4 Jul 2015 16:00	15 Aug 2016 18:00	8 Aug 2012 11:00	14 Aug 2015 00:00	8 Sep 2013 23:00	11 Sep 2017 11:00	13 Sep 2015 02:00	8 Jul 2019 04:00	5 Aug 2014 20:00
Final date	26 Aug 2017 00:00	11 Jul 2015 15:00	22 Aug 2016 17:00	15 Aug 2012 10:00	20 Aug 2015 23:00	15 Sep 2013 22:00	18 Sep 2017 10:00	20 Sep 2015 01:00	15 Jul 2019 03:00	12 Aug 2014 19:00
Autumn										
	Period 1	Period 2	Period 3	Period 4	Period 5	Period 6	Period 7	Period 8	Period 9	Period 10
Initial date	16 Oct 2014 22:00	17 Oct 2011 08:00	24 Oct 2015 11:00	8 Nov 2011 17:00	10 Dec 2020 10:00	6 Nov 2015 01:00	23 Nov 2015 21:00	4 Oct 2017 23:00	4 Oct 2015 20:00	23 Nov 2020 04:00
Final date	23 Oct 2014 21:00	24 Oct 2011 07:00	31 Oct 2015 10:00	15 Nov 2011 16:00	17 Dec 2020 09:00	13 Nov 2015 00:00	30 Nov 2015 20:00	11 Oct 2017 22:00	11 Oct 2015 19:00	30 Nov 2020 03:00

Appendix D: Seasonal mean current and wind fields (2009–2021)

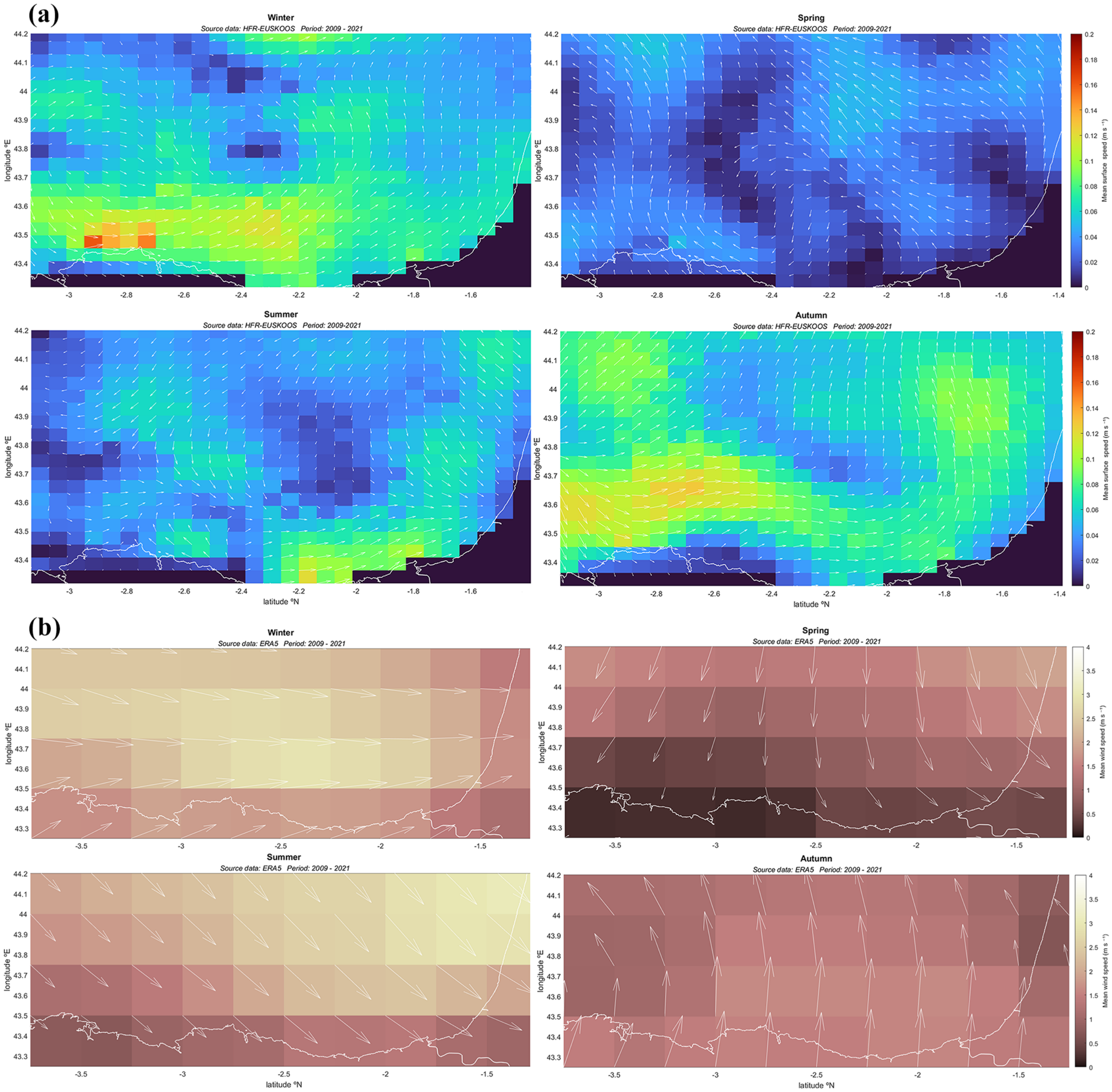

Figure D1. Mean current **(a)** and wind fields **(b)** in the study area during each season for the selected periods between 2009 and 2021. The colour bars represent the magnitude of current and wind speed. The arrows indicate the current and wind mean direction and are scaled with currents and wind speed (data sources: HF radar – EuskOOS, https://www.euskoos.eus/en/data/basque-ocean-meteorological-network/high-frequency-coastal-radars/; ERA5, https://www.ecmwf.int/en/forecasts/datasets/reanalysis-datasets/era5, last access: 11 November 2019).

Code and data availability. Code and data used to conduct this study are available upon request by contacting the corresponding authors.

Video supplement. Animations of the surface currents, winds, and Lagrangian simulations area available for the study period 2009–2021 (https://doi.org/10.5446/s_1355, Ruiz et al., 2022b).

Author contributions. IR performed the investigation, the data analysis, and the visualization assets and wrote the original paper. AJA contributed to the conceptualization of the investigation, provided the software, and reviewed and edited the paper. OCB and AR contributed to the conceptualization of the investigation and supervised, reviewed, and edited the paper. All authors contributed to refining the paper for submission.

Competing interests. The contact author has declared that none of the authors has any competing interests.

Disclaimer. Publisher's note: Copernicus Publications remains neutral with regard to jurisdictional claims in published maps and institutional affiliations.

Acknowledgements. We are grateful to the Emergencies and Meteorology Directorate – Security department – Basque Government for public data provision from the Basque Operational Oceanography System EuskOOS. This study has been conducted using EU Copernicus Marine Service information. We thank Luis Ferrer for sharing his valuable knowledge on the custom-built drifters. We thank Cristina Barreau, Antoine Bruge, Igor Granado, Théo Destang, Alix McDaid, and Jon Andonegi for their support with the release of the drifters. We thank the citizens who collected and reported the drifters' arrival at the Basque and French coasts. This paper is contribution no. 1134 from AZTI, Marine Research, Basque Research and Technology Alliance (BRTA). This paper is part of the PhD research of Irene Ruiz, supervised by Oihane C. Basurko and Anna Rubio.

Financial support. This research has been partially funded through the EU's LIFE Program (LIFE LEMA project, grant agreement no. LIFE15 ENV/ES/000252) and by the EU's H2020 Program (JERICO-S3 project, grant agreement no. 871153).

Review statement. This paper was edited by Erik van Sebille and reviewed by two anonymous referees.

References

Abascal, A., Castanedo, S., Gutierrez, A. D., Comerma, E., Medina, R., and Losada, I. J.: Teseo, an operational system for simulating oil spills trajectories and fate processes, Proc. Int. Offshore Polar Eng. Conf., 1751–1758, ISBN 978-1-880653-68-5, 2007.

Abascal, A. J., Castanedo, S., Mendez, F. J., Medina, R., and Losada, I. J.: Calibration of a Lagrangian Transport Model Using Drifting Buoys Deployed during the *Prestige* Oil Spill, J. Coastal Res., 11, 80–90, 2009.

Abascal, A. J., Castanedo, S., Fernández, V., and Medina, R.: Backtracking drifting objects using surface currents from high-frequency (HF) radar technology, Ocean Dynam., 62, 1073–1089, https://doi.org/10.1007/s10236-012-0546-4, 2012.

Abascal, A. J., Castanedo, S., Núñez, P., Mellor, A., Clements, A., Pérez, B., Cárdenas, M., Chiri, H., and Medina, R.: A high-resolution operational forecast system for oil spill response in Belfast Lough, Mar. Pollut. Bull., 114, 302–314, https://doi.org/10.1016/j.marpolbul.2016.09.042, 2017a.

Abascal, A. J., Sanchez, J., Chiri, H., Ferrer, M. I., Cárdenas, M., Gallego, A., Castanedo, S., Medina, R., Alonso-Martirena, A., Berx, B., Turrell, W. R., and Hughes, S. L.: Operational oil spill trajectory modelling using HF radar currents: A northwest European continental shelf case study, Mar. Pollut. Bull., 119, 336–350, https://doi.org/10.1016/j.marpolbul.2017.04.010, 2017b.

Aksamit, N. O., Sapsis, T., and Haller, G.: Machine-Learning Mesoscale and Submesoscale Surface Dynamics from Lagrangian Ocean Drifter Trajectories, J. Phys. Oceanogr., 50, 1179–1196, https://doi.org/10.1175/jpo-d-19-0238.1, 2020.

Al-Zawaidah, H., Ravazzolo, D., and Friedrich, H.: Macroplastics in rivers: present knowledge, issues and challenges, Environ. Sci.-Proc. Imp., 23, 535–552, https://doi.org/10.1039/d0em00517g, 2021.

Allshouse, M. R., Ivey, G. N., Lowe, R. J., Jones, N. L., Beegle-Krause, C. J., Xu, J., and Peacock, T.: Impact of windage on ocean surface Lagrangian coherent structures, Environ. Fluid Mech., 17, 473–483, https://doi.org/10.1007/s10652-016-9499-3, 2017.

ASCE: State-of-the-Art Review of Modeling Transport and Fate of Oil Spills, J. Hydraul. Eng., 122, 594–609, https://doi.org/10.1061/(ASCE)0733-9429(1996)122:11(594), 1996.

Blettler, M. C. M., Abrial, E., Khan, F. R., Sivri, N., and Espinola, L. A.: Freshwater plastic pollution: Recognizing research biases and identifying knowledge gaps, Water Res., 143, 416–424, https://doi.org/10.1016/j.watres.2018.06.015, 2018.

Bourillet, J. F., Zaragosi, S., and Mulder, T.: The French Atlantic margin and deep-sea submarine systems, Geo-Mar. Lett., 26, 311–315, https://doi.org/10.1007/s00367-006-0042-2, 2006.

Brennan, E., Wilcox, C., and Hardesty, B. D.: Connecting flux, deposition and resuspension in coastal debris surveys, Sci. Total Environ., 644, 1019–1026, https://doi.org/10.1016/J.SCITOTENV.2018.06.352, 2018.

Bruge, A., Barreau, C., Carlot, J., Collin, H., Moreno, C., and Maison, P.: Monitoring Litter Inputs from the Adour River (Southwest France) to the Marine Environment, Mar. Sci. Eng., 6, 24, https://doi.org/10.3390/jmse6010024, 2018.

C3S: ERA5: Fifth Generation of ECMWF Atmospheric Reanalyses of the Global Climate, https://cds.climate.copernicus.eu/cdsapp#!/home, last access: 11 November 2019.

Callies, U., Groll, N., Horstmann, J., Kapitza, H., Klein, H., Maßmann, S., and Schwichtenberg, F.: Surface drifters in the German Bight: model validation considering windage and Stokes drift, Ocean Sci., 13, 799–827, https://doi.org/10.5194/os-13-799-2017, 2017.

Carlson, D. F., Pavalko, W. J., Petersen, D., Olsen, M., and Hass, A. E.: Maker Buoy Variants for Water Level Monitoring and Tracking Drifting Objects in Remote Areas of Greenland, 20, 1254, https://doi.org/10.3390/s20051254, 2020.

Carson, H. S., Lamson, M. R., Nakashima, D., Toloumu, D., Hafner, J., Maximenko, N., and McDermid, K. J.: Tracking the sources and sinks of local marine debris in Hawai'i, Mar. Environ. Res., 84, 76–83, 2013.

Chamas, A., Moon, H., Zheng, J., Qiu, Y., Tabassum, T., Hee Jang, J., Abu-Omar, M., Scott, S. L., and Suh, S.: Degradation Rates of Plastics in the Environment, ACS Sustain. Chem. Eng, 8, 3511, https://doi.org/10.1021/acssuschemeng.9b06635, 2020.

Charria, G., Lazure, P., Le Cann, B., Serpette, A., Reverdin, G., Louazel, S., Batifoulier, F., Dumas, F., Pichon, A., and Morel, Y.: Surface layer circulation derived from Lagrangian drifters in the Bay of Biscay, J. Marine Syst., 109, S60–S76, https://doi.org/10.1016/j.jmarsys.2011.09.015, 2013.

Chiri, H., Abascal, A. J., Castanedo, S., and Medina, R.: Mid-long term oil spill forecast based on logistic regression modelling of met-ocean forcings, Mar. Pollut. Bull., 146, 962–976, https://doi.org/10.1016/j.marpolbul.2019.07.053, 2019.

Chiri, H., Abascal, A. J., and Castanedo, S.: Deep oil spill hazard assessment based on spatio-temporal met-ocean patterns, Mar. Pollut. Bull., 154, 111123, https://doi.org/10.1016/J.MARPOLBUL.2020.111123, 2020.

Compa, M., Alomar, C., Morató, M., Álvarez, E., and Deudero, S.: Spatial distribution of macro- and micro-litter items along rocky and sandy beaches of a Marine Protected Area in the western Mediterranean Sea, Mar. Pollut. Bull., 178, 113520, https://doi.org/10.1016/J.MARPOLBUL.2022.113520, 2022.

Critchell, K. and Lambrechts, J.: Modelling accumulation of marine plastics in the coastal zone; what are the dominant physical processes?, Estuar. Coast. Shelf S., 171, 111, https://doi.org/10.1016/j.ecss.2016.01.036, 2016.

D'Asaro, E. A., Carlson, D. F., Chamecki, M., Harcourt, R. R., Haus, B. K., Fox-Kemper, B., Molemaker, M. J., Poje, A. C., and Yang, D.: Advances in Observing and Understanding Small-Scale Open Ocean Circulation During the Gulf of Mexico Research Initiative Era, Front. Mar. Sci., 7, 349, https://doi.org/10.3389/fmars.2020.00349, 2020.

Declerck, A., Delpey, M., Rubio, A., Ferrer, L., Basurko, O. C., Mader, J., and Louzao, M.: Transport of floating marine litter in the coastal area of the south-eastern Bay of Biscay: A Lagrangian approach using modelling and observations, J. Oper. Oceanogr., 12, S111–S125, https://doi.org/10.1080/1755876x.2019.1611708, 2019.

Delpey, M., Declerck, A., Epelde, I., Voirand, T., Manso-Navarte, I., Mader, J., Rubio, A., and Caballero, A.: Tracking floating marine litter in the coastal area by combining operational ocean modelling and remote observation systems., EGU General Assembly 2021, online, 19–30 Apr 2021, EGU21-11465, https://doi.org/10.5194/egusphere-egu21-11465, 2021.

Duhec, A. V., Jeanne, R. F., Maximenko, N., and Hafner, J.: Composition and potential origin of marine debris stranded in the Western Indian Ocean on remote Alphonse Island, Seychelles, Mar. Pollut. Bull., 96, 76–86, https://doi.org/10.1016/j.marpolbul.2015.05.042, 2015.

European Commission (Joint Research Centre, Addamo, A., Laroche, P., Hanke, G.): Top marine beach litter items in Europe, European Commission, Joint Research Centre, Publications Office of the European Union, https://doi.org/10.2760/496717, 2018.

Eurostat: Population density by NUTS 3 region, http://data.europa.eu/88u/dataset/gngfvpqmfu5n6akvxqkpw (last access: 21 February 2020), 2019.

Fazey, F. M. C. and Ryan, P. G.: Biofouling on buoyant marine plastics: An experimental study into the effect of size on surface longevity, Environ. Pollut., 210, 354–360, https://doi.org/10.1016/J.ENVPOL.2016.01.026, 2016.

Ferrer, L. and Pastor, A.: The Portuguese man-of-war: Gone with the wind, Reg. Stud. Mar. Sci., 14, 53–62, https://doi.org/10.1016/j.rsma.2017.05.004, 2017.

Gasperi, J., Dris, R., Bonin, T., Rocher, V., and Tassin, B.: Assessment of floating plastic debris in surface water along the Seine River, Environ. Pollut., 195, 163–166, https://doi.org/10.1016/j.envpol.2014.09.001, 2014.

González, M., Valencia, V., Mader, J., Fontán, A., Uriarte, A., and Caballero, A.: Operational Coastal Systems in the Basque Country Region: Modelling and Observations, Seventeenth International Offshore and Polar Engineering Conference, Lisbon, Portugal, 1 July 2007, Proc. Int. Offshore Polar Eng. Conf., ISOPE-I-07-074, 2007.

González-Fernández, D. and Hanke, G.: Toward a Harmonized Approach for Monitoring of Riverine Floating Macro Litter Inputs to the Marine Environment, Front. Mar. Sci., 4, 86, https://doi.org/10.3389/fmars.2017.00086, 2017.

González-Fernández, D., Hanke, G., Kideys, A., Navarrao Ortega, A., Sanchez Vidal, A., Bruge, A., Öztürk, B., Palma, C., Santelli, C., Duijsings, D., Barcelo, D., Dimitiriu, E., Rojo-Nieto, E., Ferreira, F., Bessa, F., Suaria, G., Siedlewicz, G., Castro Jimenez, J., Germano, J., Pereira De Brito, J., Rigueira, J., Pazdro, K., Cabrera, M., Pogojeva, M., Köck Schulmeyer, M., Constant, M., Canals Artigas, M., Paraboschi, M., Tourgeli, M., Machitadze, N., Ratola, N., Savenko, O., Kerherve, P., Sempere, R., Bakiu, R., Crosti, R., Schoeneich-Argent, R., Landry Levesque, S., Agostinho, T., Segal, Y., and Galletti, Y.: Floating Macro Litter in European Rivers – Top Items, EUR 29383 EN, Publications Office of the European Union, Luxembourg, https://doi.org/10.2760/316058, 2018.

González-Fernández, D., Cózar, A., Hanke, G., Viejo, J., Morales-Caselles, C., Bakiu, R., Barceló, D., Bessa, F., Bruge, A., Cabrera, M., Castro-Jiménez, J., Constant, M., Crosti, R., Galletti, Y., Kideys, A. E., Machitadze, N., Pereira de Brito, J., Pogojeva, M., Ratola, N., Rigueira, J., Rojo-Nieto, E., Savenko, O., Schöneich-Argent, R. I., Siedlewicz, G., Suaria, G., and Tourgeli, M.: Floating macrolitter leaked from Europe into the ocean, Nat. Sustain., 4, 474–483, https://doi.org/10.1038/s41893-021-00722-6, 2021.

Haza, A. C., Paldor, N., Özgökmen, T. M., Curcic, M., Chen, S. S., and Jacobs, G.: Wind-Based Estimations of Ocean Surface Currents From Massive Clusters of Drifters in the Gulf of Mexico, J. Geophys. Res.-Oceans, 124, 5844–5869, https://doi.org/10.1029/2018JC014813, 2019.

Hernández-Carrasco, I., Solabarrieta, L., Rubio, A., Esnaola, G., Reyes, E., and Orfila, A.: Impact of HF radar current gap-filling methodologies on the Lagrangian assessment of coastal dynamics, Ocean Sci., 14, 827–847, https://doi.org/10.5194/os-14-827-2018, 2018.

Hoenner, X., Barlian, E., Ernawati, T., Hardesty, B. D., Kembaren, D. D., Mous, P. J., Sadiyah, L., Satria, F., and Wilcox, C.: Using anti-theft tracking devices to infer fishing vessel activity at sea, Fish. Res., 249, 106230, https://doi.org/10.1016/j.fishres.2022.106230, 2022.

Hunter, J. R., Craig, P. D., and Phillips, H. E.: On the use of random walk models with spatially variable diffusivity, J. Comput. Phys., 106, 366–376, https://doi.org/10.1016/S0021-9991(83)71114-9, 1993.

Joint Research Centre (Institute for Environment and Sustainability): Guidance on monitoring of marine litter in European seas, Publications Office, https://doi.org/10.2788/99816, 2014.

Kaplan, D. M. and Lekien, F.: Spatial interpolation and filtering of surface current data based on open-boundary modal analysis, J. Geophys. Res.-Oceans, 112, C12007, https://doi.org/10.1029/2006JC003984, 2007.

Karagiorgos, J., Vervatis, V., and Sofianos, S.: The Impact of Tides on the Bay of Biscay Dynamics, J. Mar. Sci. Eng., 8, 617, https://doi.org/10.3390/jmse8080617, 2020.

Ko, C.-Y., Hsin, Y.-C., and Jeng, M.-S.: Global distribution and cleanup opportunities for macro ocean litter: a quarter century of accumulation dynamics under windage effects, Environ. Res. Lett., 15, 104063, https://doi.org/10.1088/1748-9326/abae29, 2020.

Kooi, M., Nes, E. H. van, Scheffer, M., and Koelmans, A. A.: Ups and Downs in the Ocean: Effects of Biofouling on Vertical Transport of Microplastics, Environ. Sci. Technol., 51, 7963–7971, https://doi.org/10.1021/acs.est.6b04702, 2017.

Lavin, A., Valdés, L., Sanchez, F., Abaunza, P., Forest, A., Boucher, J., Lazure, P., and Jegou, A.-M.: The Bay of Biscay: the encountering of the Ocean and the Shelf (18b, E), edited by: Robinson, A. and Brink, K., Combridge, MA, Harvard University Press, http://hdl.handle.net/10508/3128 (last access: 25 November 2022) 2006.

Le Boyer, A., Charria, G., Le Cann, B., Lazure, P., and Marié, L.: Circulation on the shelf and the upper slope of the Bay of Biscay, Cont. Shelf Res., 55, 97–107, 2013.

Lebreton, L. C. M., Greer, S. D., and Borrero, J. C.: Numerical modelling of floating debris in the world's oceans, Mar. Pollut. Bull., 64, 653–661, 2012.

Lebreton, L., Egger, M., and Slat, B.: A global mass budget for positively buoyant macroplastic debris in the ocean, Sci. Rep.-UK, 9, 12922, https://doi.org/10.1038/s41598-019-49413-5, 2019.

Lebreton, L. C. M., van der Zwet, J., Damsteeg, J.-W., Slat, B., Andrady, A., and Reisser, J.: River plastic emissions to the world's oceans, Nat. Commun., 8, 15611, https://doi.org/10.1038/ncomms15611, 2017.

Lechner, A., Keckeis, H., Lumesberger-Loisl, F., Zens, B., Krusch, R., Tritthart, M., Glas, M., and Schludermann, E.: The Danube so colourful: A potpourri of plastic litter outnumbers fish larvae in Europe's second largest river, Environ. Pollut., 188, 177–181, https://doi.org/10.1016/J.ENVPOL.2014.02.006, 2014.

Maclean, K., Weideman, E. A., Perold, V., and Ryan, P. G.: Buoyancy affects stranding rate and dispersal distance of floating litter entering the sea from river mouths, Mar. Pollut. Bull., 173, 113028, https://doi.org/10.1016/j.marpolbul.2021.113028, 2021.

Mai, L., Sun, X., Xia, L.-L., Bao, L.-J., Liu, L.-Y., and Zeng, E. Y.: Global Riverine Plastic Outflows, Environ. Sci. Technol., 54, 10049–10056, https://doi.org/10.1021/acs.est.0c02273, 2020.

Maier-Reimer, E. and Sündermann, J.: On tracer methods in computational hydrodynamics, in: Engineering applications of computational hydraulics, edited by: Abbott, M. B., 198–216, https://hdl.handle.net/21.11116/0000-0004-F582-4 (last access: 25 November 2022), 1982.

Manso-Narvarte, I., Caballero, A., Rubio, A., Dufau, C., and Birol, F.: Joint analysis of coastal altimetry and high-frequency (HF) radar data: observability of seasonal and mesoscale ocean dynamics in the Bay of Biscay, Ocean Sci., 14, 1265–1281, https://doi.org/10.5194/os-14-1265-2018, 2018.

Manso-Narvarte, I., Rubio, A., Jordà, G., Carpenter, J., Merckelbach, L., and Caballero, A.: Three-Dimensional Characterization of a Coastal Mode-Water Eddy from Multiplatform Observations and a Data Reconstruction Method, Remote Sens., 13, 674, https://doi.org/10.3390/rs13040674, 2021.

Mantovani, C., Corgnati, L., Horstmann, J., Rubio, A., Reyes, E., Quentin, C., Cosoli, S., Asensio, J. L., Hermes, J., Mader, J., and Griffa, A.: Best Practices on High Frequency Radar Deployment and Operation for Ocean Current Measurement, Front. Mar. Sci., 7, 210, https://doi.org/10.3389/fmars.2020.00210, 2020.

Margenat, H., Ruiz-Orejón, L. F., Cornejo, D., Martí, E., Vila, A., Le Roux, G., Hansson, S., and Guasch, H.: Guidelines of field-tested procedures and methods for monitoring plastic litter in Mountain riverine systems, European Commission, https://doi.org/10.20350/digitalCSIC/13880, 2021.

Marta-Almeida, M., Ruiz-Villarreal, M., Pereira, J., Otero, P., Cirano, M., Zhang, X., and Hetland, R. D.: Efficient tools for marine operational forecast and oil spill tracking, Mar. Pollut. Bull., 71, 139–151, https://doi.org/10.1016/J.MARPOLBUL.2013.03.022, 2013.

Martínez Fernández, A., Redondo Caride, W., Alonso Pérez, F., Piedracoba Varela, S., Lorente Jiménez, P., Montero Vilar, P., Torres López, S., Fernández Baladrón, A., Varela Benvenuto, R. A., and Velo Lanchas, A.: SPOT and GPRS drifting buoys for HF Radar calibration, Instrum. Viewp., Universidad Politécnica de Cataluña, 48–49, http://hdl.handle.net/10261/259925 (last access: 25 November 2022), 2021.

Maximenko, N., Hafner, J., Kamachi, M., and MacFadyen, A.: Numerical simulations of debris drift from the Great Japan Tsunami of 2011 and their verification with observational reports, Mar. Pollut. Bull., 132, 5–25, https://doi.org/10.1016/j.marpolbul.2018.03.056, 2018.

Mazarrasa, I., Puente, A., Núñez, P., García, A., Abascal, A. J., and Juanes, J. A.: Assessing the risk of marine litter accumulation in estuarine habitats, Mar. Pollut. Bull., 144, 117–128, https://doi.org/10.1016/j.marpolbul.2019.04.060, 2019.

Meijer, L. J. J., van Emmerik, T., van der Ent, R., Schmidt, C., and Lebreton, L.: More than 1000 rivers account for 80 % of global riverine plastic emissions into the ocean, Sci. Adv., 7, eaaz5803, https://doi.org/10.1126/sciadv.aaz5803, 2021.

Melvin, J., Bury, M., Ammendolia, J., Charles, M., and Liboiron, M.: Critical Gaps in Shoreline Plastics Pollution Research, Front. Mar. Sci., 8, 689108, https://doi.org/10.3389/fmars.2021.689108, 2021.

Meyerjürgens, J., Badewien, T. H., Garaba, S. P., Wolff, J.-O., and Zielinski, O.: A State-of-the-Art Compact Surface Drifter Reveals Pathways of Floating Marine Litter in the German Bight, Front. Mar. Sci., 6, 58, https://doi.org/10.3389/fmars.2019.00058, 2019.

Min, K., Cuiffi, J. D., and Mathers, R. T.: Ranking environmental degradation trends of plastic marine debris based on physical properties and molecular structure, Nat. Commun., 11, 727, https://doi.org/10.1038/s41467-020-14538-z, 2020.

Neumann, D., Callies, U., and Matthies, M.: Marine litter ensemble transport simulations in the southern North Sea, Mar. Pollut. Bull., 86, 219–228, https://doi.org/10.1016/j.marpolbul.2014.07.016, 2014.

Novelli, G., Guigand, C. M., Cousin, C., Ryan, E. H., Laxague, N. J. M., Dai, H., Haus, B. K., and Özgökmen, T. M.: A Biodegradable Surface Drifter for Ocean Sampling on a Massive Scale, J. Atmos. Ocean. Tech., 34, 2509–2532, https://doi.org/10.1175/jtech-d-17-0055.1, 2017.

Novelli, G., Guigand, C. M., and Özgökmen, T. M.: Technological Advances in Drifters for Oil Transport Studies, Mar. Technol. Soc. J., 52, 53–61, https://doi.org/10.4031/mtsj.52.6.9, 2018.

Núñez, P., García, A., Mazarrasa, I., Juanes, J. A., Abascal, A. J., Méndez, F., Castanedo, S., and Medina, R.: A methodology to assess the probability of marine litter accumulation in estuaries, Mar. Pollut. Bull., 144, 309–324, https://doi.org/10.1016/j.marpolbul.2019.04.077, 2019.

Ocio, D., Stocker, C., Eraso, A., and Cowpertwait, P.: Regionalized extreme flows by means of stochastic storm generation coupled with a distributed hydrological model. The case of the Basque Country, Proc. 36th IAHR World Congr., 28 June–3 July 2015, 1–13, https://doi.org/10.13140/RG.2.1.3924.4889, 2015.

Pereiro, D., Souto, C., and Gago, J.: Calibration of a marine floating litter transport model, J. Oper. Oceanogr., 11, 125–133, https://doi.org/10.1080/1755876x.2018.1470892, 2018.

Pereiro, D., Souto, C., and Gago, J.: Dynamics of floating marine debris in the northern Iberian waters: A model approach, J. Sea Res., 144, 57–66, https://doi.org/10.1016/j.seares.2018.11.007, 2019.

Porter, M., Inall, M. E., Green, J. A. M., Simpson, J. H., Dale, A. C., and Miller, P. I.: Drifter observations in the summer time Bay of Biscay slope current, J. Marine Syst., 157, 65–74, 2016.

Puillat, I., Lazure, P., Anne-marie, J., Lampert, L., and Miller, P.: Mesoscale hydrological variability induced by northwesterly wind on the French continental shelf of the Bay of Biscay, Sci. Mar., 70, 15–26, 2006.

Putman, N. F., Lumpkin, R., Olascoaga, M. J., Trinanes, J., and Goni, G. J.: Improving transport predictions of pelagic Sargassum, J. Exp. Mar. Biol. Ecol., 529, 151398, https://doi.org/10.1016/j.jembe.2020.151398, 2020.

Reed, M., Turner, C., and Odulo, A.: The role of wind and emulsification in modelling oil spill and surface drifter trajectories, Spill Sci. Technol. B., 1, 143–157, https://doi.org/10.1016/1353-2561(94)90022-1, 1994.

Révelard, A., Reyes, E., Mourre, B., Hernández-Carrasco, I., Rubio, A., Lorente, P., Fernández, C. D. L., Mader, J., Álvarez-Fanjul, E., and Tintoré, J.: Sensitivity of Skill Score Metric to Validate Lagrangian Simulations in Coastal Areas: Recommendations for Search and Rescue Applications, Front. Mar. Sci., 8, 630388, https://doi.org/10.3389/fmars.2021.630388, 2021.

Rizal, A., Gautama, B. G., Pranowo, W. S., Farhan, A. R., Siong, K., Harjono, M. R., Voisin, J. B., Maes, C., Dobler, D., Berlianty, D., Priyono, B., Dufau, C., Lucas, M., Fauny, O., and Rahmania, R.: Tracking the Stranded Area of Marine Debris in Indonesian coasts by using Floating Drifter, IOP Conf. Ser.-Earth Environ. Sci., 925, 12034, https://doi.org/10.1088/1755-1315/925/1/012034, 2021.

Robbe, E., Woelfel, J., Balčiūnas, A., and Schernewski, G.: An Impact Assessment of Beach Wrack and Litter on Beach Ecosystem Services to Support Coastal Management at the Baltic Sea, Environ. Manage., 68, 835–859, https://doi.org/10.1007/s00267-021-01533-3, 2021.

Rodríguez, J. G., Garmendia, J. M., Muxika, I., Gómez-Ballesteros, M., Quincoces, I., Díez, I., Arrese, B., Sánchez, F., and Galparsoro, I.: Macrofaunal variability in the continental shelf and canyons in the southeastern Bay of Biscay, Reg. Stud. Mar. Sci., 48, 102012, https://doi.org/10.1016/j.rsma.2021.102012, 2021.

Rodríguez-Díaz, L., Gómez-Gesteira, J. L., Costoya, X., Gómez-Gesteira, M., and Gago, J.: The Bay of Biscay as a trapping zone for exogenous plastics of different sizes, J. Sea Res., 163, 101929, https://doi.org/10.1016/j.seares.2020.101929, 2020.

Rubio, A., Reverdin, G., Fontán, A., González, M., and Mader, J.: Mapping near-inertial variability in the SE Bay of Biscay from HF radar data and two offshore moored buoys, Geophys. Res. Lett., 38, 1–6, https://doi.org/10.1029/2011GL048783, 2011.

Rubio, A., Solabarrieta, L., Gonzalez, M., Mader, J., Castanedo, S., Medina, R., Charria, G., and Aranda, J. A.: Surface circulation and Lagrangian transport in the SE Bay of Biscay from HF radar data, Ocean. 2013 MTS/IEEE Bergen Challenges North. Dimens., https://doi.org/10.1109/OCEANS-Bergen.2013.6608039, 2013.

Rubio, A., Mader, J., Corgnati, L., Mantovani, C., Griffa, A., Novellino, A., Quentin, C., Wyatt, L., Schulz-Stellenfleth, J., Horstmann, J., Lorente, P., Zambianchi, E., Hartnett, M., Fernandes, C., Zervakis, V., Gorringe, P., Melet, A., and Puillat, I.: HF Radar Activity in European Coastal Seas: Next Steps toward a Pan-European HF Radar Network, Front. Mar. Sci., 4, 8, https://doi.org/10.3389/fmars.2017.00008, 2017.

Rubio, A., Caballero, A., Orfila, A., Hernández-Carrasco, I., Ferrer, L., González, M., Solabarrieta, L., and Mader, J.: Eddy-induced cross-shelf export of high Chl-*a* coastal waters in the SE Bay of Biscay, Remote Sens. Environ., 205, 290–304, https://doi.org/10.1016/j.rse.2017.10.037, 2018.

Rubio, A., Hernández-Carrasco, I., Orfila, A., González, M., Reyes, E., Corgnati, L., Berta, M., Griffa, A., and Mader, J.: A Lagrangian approach to monitor local particle retention conditions in coastal areas, J. Oper. Oceanogr., 13, S1–S172, https://doi.org/10.1080/1755876X.2020.1785097, 2020.

Ruiz, I., Basurko, O. C., Rubio, A., Delpey, M., Granado, I., Declerck, A., Mader, J., and Cózar, A.: Litter Windrows in the South-East Coast of the Bay of Biscay: An Ocean Process Enabling Effective Active Fishing for Litter, Front. Mar. Sci., 7, 308, https://doi.org/10.3389/fmars.2020.00308, 2020.

Ruiz, I., Abascal, A. J., Basurko, O. C., and Rubio, A.: Modelling the distribution of fishing-related floating marine litter within the Bay of Biscay and its marine protected areas, Environ. Pollut., 292, 118216, https://doi.org/10.1016/j.envpol.2021.118216, 2022a.

Ruiz, I., Rubio, A., Abascal, A. J., and Basurko, O. C.: Supplemental videos of the paper "Modelling floating riverine litter in the south-eastern Bay of Biscay: a regional distribution from a seasonal perspective", TIB [video], https://doi.org/10.5446/s_1355, 2022b.

Russell, K.: Spain's Coastal Authority Uses Spot Trace for Search and Rescue Training, https://www.satellitetoday.com/telecom/2017/06/20/spains-coastal-authority-uses-spot-trace-search-rescue-training/ (last access: 21 December 2019), 2017.

Ryan, P. G.: Does size and buoyancy affect the long-distance transport of floatingdebris?, Environ. Res. Lett., 10, 1, https://doi.org/10.1088/1748-9326/10/8/084019, 2015.

Schmidt, C., Krauth, T., and Wagner, S.: Export of Plastic Debris by Rivers into the Sea, Environ. Sci. Technol., 51, 12246–12253, https://doi.org/10.1021/acs.est.7b02368, 2017.

Schuyler, Q., Wilcox, C., Lawson, T. J., Ranatunga, R. R. M. K. P., Hu, C.-S., Global Plastics Project Partners, and Hardestey, B. D.: Human Population Density is a Poor Predictor of Debris in the Environment, Front. Environ. Sci., 9, 583454, https://doi.org/10.3389/fenvs.2021.583454, 2021.

Sheppard, C.: World Seas: An Environmental Evaluation: Volume I: Europe, The Americas and West Africa, edited by: Sheppard, C., Academic press, Elsevier, https://doi.org/10.1016/C2015-0-04330-1, 2018.

Solabarrieta, L., Rubio, A., Castanedo, S., Medina, R., Charria, G., and Hernández, C.: Surface water circulation patterns in the southeastern Bay of Biscay: New evidences from HF radar data, Cont. Shelf Res., 74, 60–76, https://doi.org/10.1016/j.csr.2013.11.022, 2014.

Solabarrieta, L., Rubio, A., Cárdenas, M., Castanedo, S., Esnaola, G., Méndez, F. J., Medina, R., and Ferrer, L.: Probabilistic relationships between wind and surface water circulation patterns in the SE Bay of Biscay, Ocean Dynam., 65, 1289–1303, https://doi.org/10.1007/s10236-015-0871-5, 2015.

Solabarrieta, L., Frolov, S., Cook, M., Paduan, J., Rubio, A., González, M., Mader, J., and Charria, G.: Skill Assessment of HF Radar–Derived Products for Lagrangian Simulations in the Bay of Biscay, J. Atmos. Ocean. Tech., 33, 2585–2597, https://doi.org/10.1175/jtech-d-16-0045.1, 2016.

Solabarrieta, L., Hernández-Carrasco, I., Rubio, A., Campbell, M., Esnaola, G., Mader, J., Jones, B. H., and Orfila, A.: A new Lagrangian-based short-term prediction methodology for high-frequency (HF) radar currents, Ocean Sci., 17, 755–768, https://doi.org/10.5194/os-17-755-2021, 2021.

Stanev, E. V., Badewien, T. H., Freund, H., Grayek, S., Hahner, F., Meyerjürgens, J., Ricker, M., Schöneich-Argent, R. I., Wolff, J. O., and Zielinski, O.: Extreme westward surface drift in the North Sea: Public reports of stranded drifters and Lagrangian tracking, Cont. Shelf Res., 177, 24–32, https://doi.org/10.1016/j.csr.2019.03.003, 2019.

Teles-Machado, A., Peliz, Á., McWilliams, J. C., Dubert, J., and Cann, B. Le: Circulation on the Northwestern Iberian Margin: Swoddies, Prog. Oceanogr., 140, 116–133, https://doi.org/10.1016/J.POCEAN.2015.09.011, 2016.

Tong, X., Jong, M.-C., Zhang, J., You, L., and Gin, K. Y.-H.: Modelling the spatial and seasonal distribution, fate and transport of floating plastics in tropical coastal waters, J. Hazard. Mater., 414, 125502, https://doi.org/10.1016/j.jhazmat.2021.125502, 2021.

Van Der Mheen, M., Pattiaratchi, C., and Van Sebille, E.: Role of Indian Ocean Dynamics on Accumulation of Buoyant Debris, J. Geophys. Res.-Oceans, 124, 2571–2590, https://doi.org/10.1029/2018JC014806, 2019.

van der Wal, M., van der Meulen, M., Tweehuijsen, G., Peterlin, M., Palatinus, A., Kovač Viršek, M., Coscia, L., and Kržan, A.: Identification and Assessment of Riverine Input of (Marine) Litter, Final Rep. Eur. Comm. DG Environ. under Framew. Contract No. ENV.D.2/FRA/2012/0025, 1–208, 2015.

van Emmerik, T. and Schwarz, A.: Plastic debris in rivers, WIREs Water, 7, e1398, https://doi.org/10.1002/wat2.1398, 2020.

van Sebille, E., England, M. H., and Froyland, G.: Origin, dynamics and evolution of ocean garbage patches from observed surface drifters, Environ. Res. Lett., 7, 044040, https://doi.org/10.1088/1748-9326/7/4/044040, 2012.

Van Sebille, E., Aliani, S., Law, K. L., Maximenko, N., Alsina, J. M., Bagaev, A., Bergmann, M., Chapron, B., Chubarenko, I., and Cózar, A.: The physical oceanography of the transport of floating marine debris, Environ. Res. Lett., 15, 23003, https://doi.org/10.1088/1748-9326/ab6d7d, 2020.

van Sebille, E., Zettler, E., Wienders, N., Amaral-Zettler, L., Elipot, S., and Lumpkin, R.: Dispersion of Surface Drifters in the Tropical Atlantic, Front. Mar. Sci., 7, 607426, https://doi.org/10.3389/fmars.2020.607426, 2021.

van Utenhove, E.: Modelling the transport and fate of buoyant macroplastics in coastal waters, Master thesis, http://resolver.tudelft.nl/uuid:be6a41d2-6071-47b9-926d-f22c23edadba (last access: 25 November 2022), 2019.

Weideman, E. A., Perold, V., Omardien, A., Smyth, L. K., and Ryan, P. G.: Quantifying temporal trends in anthropogenic litter in a rocky intertidal habitat, Mar. Pollut. Bull., 160, 111543, https://doi.org/10.1016/J.MARPOLBUL.2020.111543, 2020.

Wendt-Potthoff, K., Avellán, T., van Emmerik, T., Hamester, M., Kirschke, S., Kitover, D., and Schmidt, C.: Monitoring Plastics in Rivers and Lakes: Guidelines for the Harmonization of Methodologies, edited by: Smith, J., United Nations Environment Programme, ISBN 9789280738193, 2020.

Widyatmoko, A. C., Hardesty, B. D., and Wilcox, C.: Detecting anchored fish aggregating devices (AFADs) and estimating use patterns from vessel tracking data in small-scale fisheries, Sci. Rep.-UK, 11, 17909, https://doi.org/10.1038/s41598-021-97227-1, 2021.

Woods, J. S., Verones, F., Jolliet, O., Vázquez-Rowe, I., and Boulay, A.-M.: A framework for the assessment of marine litter impacts in life cycle impact assessment, Ecol. Indic., 129, 107918, https://doi.org/10.1016/j.ecolind.2021.107918, 2021.

Yoon, J.-H., Kawano, S., and Igawa, S.: Modeling of marine litter drift and beaching in the Japan Sea, Mar. Pollut. Bull., 60, 448, https://doi.org/10.1016/j.marpolbul.2009.09.033, 2010.